

1 **Selective Impact of ALK and MELK Inhibition on ER α Stability and Cell Proliferation in**
2 **Cell Lines Representing Distinct Molecular Phenotypes of Breast Cancer**

3
4 Stefania Bartoloni¹, Sara Pescatori¹, Fabrizio Bianchi², Manuela Cipolletti¹, and Filippo Acconcia^{1*}.

5
6 ¹Department of Sciences, Section Biomedical Sciences and Technology, University Roma Tre,
7 Rome, Italy. ²Fondazione IRCCS Casa Sollievo della Sofferenza, Cancer Biomarkers Unit, 71013
8 San Giovanni Rotondo (FG), Italy.
9

10
11
12
13
14
15
16
17
18
19
20
21
22
23
24
25
26
27
28
29
30
31
32
33
34
35
36
37
38
39
40
41
42
43
44
45
46
47
48
49 * Correspondence should be addressed to Prof Filippo Acconcia, filippo.acconcia@uniroma3.it at the
50 Department of Sciences, University Roma Tre, Viale Guglielmo Marconi, 446, I-00146, Rome, Italy.
51 Tel.: +39 0657336320; Fax: +39 0657336321.

1 **Abstract**

2 Breast cancer (BC) is a leading cause of global cancer-related mortality in women, necessitating
3 accurate tumor classification for timely intervention. Molecular and histological factors, including
4 PAM50 classification, estrogen receptor α (ER α), breast cancer type 1 susceptibility protein
5 (BRCA1), progesterone receptor (PR), and HER2 expression, contribute to intricate BC subtyping.
6 Through in silico screenings and multiple BC cell line investigations, we identified enhanced
7 sensitivity of ER α -positive BC cell lines to ALK and MELK inhibitors, inducing ER α degradation
8 and diminishing proliferation in specific BC subtypes. MELK inhibition attenuated ER α
9 transcriptional activity, impeding E2-induced gene expression, and hampering proliferation in MCF-
10 7 cells. Synergies between MELK inhibition with 4OH-tamoxifen (Tam) and ALK inhibition with
11 HER2 inhibitors revealed potential therapeutic avenues for ER α -positive/PR-positive/HER2-
12 negative and ER α -positive/PR-negative/HER2-positive tumors, respectively. Our findings propose
13 MELK as a promising target for ER α -positive/PR-positive/HER2-negative BC and highlight ALK as
14 a potential focus for ER α -positive/PR-negative/HER2-positive BC. The synergistic anti-proliferative
15 effects of MELK with Tam and ALK with HER2 inhibitors underscore kinase inhibitors' potential
16 for selective treatment in diverse BC subtypes, paving the way for personalized and effective
17 therapeutic strategies in BC management.

18 **Keywords:** MELK, ALK, ER α , breast cancer, 17 β -estradiol, personalized medicine approach, drug
19 discovery.
20

1 Introduction

2 Breast cancer (BC) remains the most lethal neoplastic disease affecting women worldwide.
3 Early diagnosis requires the accurate classification of mammary tumors to determine the appropriate
4 pharmacological approach, based on various criteria. The classification of breast tumors involves the
5 molecular expression of specific genes using the PAM50 classification, which categorizes them into
6 five clinicopathological surrogates: luminal A (LumA), luminal B (LumB), HER2-overexpressing
7 (HER2+), basal epithelial-like (BL), and normal-like (NL). Additionally, the histological type of the
8 tumor (e.g., invasive ductal carcinoma - IDC, adenocarcinoma, papillary carcinoma) is an important
9 tool for characterizing mammary carcinomas. Several key prognostic factors for BC include the
10 expression of estrogen receptor α (ER α), which distinguishes tumors as ER α -positive or ER α -
11 negative, the status of breast cancer type 1 susceptibility protein (BRCA1) (wild type – wt versus
12 mutated), and the expression of progesterone receptor (PR) and HER2, further dividing different
13 subgroups within the LumA and LumB phenotypes. However, there is some overlap between tumor
14 classifications, as any histological tumor type can be both ER α -positive and ER α -negative and belong
15 to different clinical surrogates of BC. For example, LumA tumors (PR-positive/HER2-negative; PR-
16 negative/HER2-negative) and LumB tumors (PR-negative/HER2-positive; PR-positive/HER2-
17 positive) are ER α -positive, while the other subtypes are ER α -negative, and BRCA1-mutated
18 carcinomas do not express ER α , but all of them can originate from various histological types¹⁻⁴.
19 Therefore, BC includes a variety of different molecular and biological phenotypes that make it a
20 jumble of single intrinsically different diseases.

21 Upon diagnosis, approximately 70% of newly detected breast tumors express ER α and exhibit
22 a more favorable prognosis compared to ER α -negative tumors. This is attributed to the fact that ER α
23 serves as the pharmacological target for ER α -positive tumors, which are treated with endocrine
24 therapy drugs that hinder various aspects of the 17 β -estradiol (E2):ER α signaling pathway to impede
25 cell proliferation. Patients are prescribed either aromatase inhibitors (AIs) to suppress E2 production,
26 selective estrogen receptor modulators (SERMs) like 4OH-Tamoxifen (Tam) to inhibit ER α
27 transcriptional activity, or selective estrogen receptor down-regulators (SERDs) such as fulvestrant
28 to induce ER α 26S proteasome-dependent degradation¹⁻⁴. However, LumA and LumB tumors show
29 different sensitivities to ET drugs. Tam is the primary clinical treatment for LumA tumors, whereas
30 LumB tumors, which express HER2, necessitate combination therapy involving Tam along with
31 drugs targeting this additional molecular target (e.g., gefitinib - Gef, lapatinib - Lapa, and erlotinib -
32 Erlo)^{4,5}. Therefore, the correct classification of the mammary tumor determines the specific
33 pharmacological approach for patients.

34 Despite the established effectiveness, ongoing treatment of patients with ET results in the
35 development of drug-resistant tumors in approximately 50% of cases, leading to relapse and
36 metastatic recurrence in distant organs. Metastatic breast cancer (MBC) cells, which retain ER α
37 expression, do not respond to ET drugs and prove exceedingly challenging to treat, often resulting in
38 a fatal outcome. Furthermore, different subtypes of MBC exist, representing distinct diseases and
39 contributing to the increased variability of overall BC phenotypes¹⁻⁵.

40 The substantial heterogeneity of BC and MBC phenotypes, coupled with the development of
41 resistance to ET drugs, underscores the need to identify novel therapeutics that selectively target
42 specific BC subtypes. Such drugs would either prevent the emergence of drug resistance or effectively
43 combat metastatic disease. Recently, our research has demonstrated that drugs capable of inducing
44 ER α degradation through diverse mechanisms inhibit BC cell proliferation. This finding has allowed
45 us to identify several Food and Drug Administration (FDA)-approved drugs, initially designed for
46 different purposes, which possess 'anti-estrogen-like' properties, inducing ER α degradation and
47 effectively halting the proliferation of BC cell lines⁶⁻¹⁴.

1 Interestingly, among the identified drugs, we found that the anti-proliferative effects of cardiac
2 glycosides (CG) ouabain and digoxin are more pronounced in ER α -positive BC cell lines compared
3 to ER α -negative ones, primarily due to their ability to induce ER α degradation^{6,10}. These findings
4 suggest that ER α -positive breast tumor cells might exhibit higher sensitivity to specific drugs
5 compared to ER α -negative breast tumor cells, as these drugs induce the degradation of ER α , a
6 transcription factor crucial for the G1 to S phase progression of the cell cycle¹⁵. Additionally, we
7 made an unexpected discovery that the GART inhibitor lometrexol is effective only in LumA IDC
8 cells, which mimic both primary and metastatic BC¹⁶, while the CHK1 inhibitors AZD7762 and
9 prexasertib lead to ER α degradation and prevent the proliferation of cell lines mimicking the LumA
10 but not the LumB tumor phenotype¹⁷. Therefore, drugs inducing ER α degradation can specifically
11 reduce the proliferation of certain BC subtypes.

12 This evidence suggests the existence of drugs inducing ER α degradation that could exhibit
13 enhanced sensitivity in ER α -positive compared to ER α -negative breast tumor cells and could
14 selectively target specific subtypes of ER α -positive BC. To explore this hypothesis, we conducted
15 experimental investigations utilizing a combination of screenings in silico and across various BC cell
16 lines. Our findings revealed that the inhibition of anaplastic lymphoma kinase (ALK) and maternal
17 embryonic leucine zipper kinase (MELK) selectively induces ER α degradation and prevents the
18 proliferation of cell lines representing the LumB ER α -positive/PR-negative/HER2-positive and
19 LumA ER α -positive/PR-positive/HER2-negative molecular phenotypes of BC, respectively.

20 **Results**

21 Identification of ALK as a kinase regulating ER α stability.

22 We employed an unbiased approach to identify drugs with increased sensitivity in ER α -positive
23 breast cancer (BC) cell lines compared to ER α -negative ones. Our investigation involved analyzing
24 the DepMap portal (<https://depmap.org/portal/>), which contains data on approximately 4600 drugs
25 and their effects on the cell proliferation of 26 BC cell lines. Each drug's sensitivity in specific BC
26 cell lines is represented by a numerical value in the DepMap portal. To stratify the BC cell lines based
27 on ER α expression, we utilized previous molecular characterizations of the BC cell lines^{18,19}. For
28 each drug, we calculated the mean sensitivity value in both ER α -positive and ER α -negative BC cell
29 lines. Then, we determined the difference in mean sensitivity between ER α -positive and ER α -
30 negative BC cell lines for each drug. Using a Student t-test, we estimated the relative p-values, which
31 were subsequently -Log₂ transformed. We visualized the results in a Volcano plot, revealing that the
32 majority of drugs in the DepMap database exhibited increased sensitivity in ER α -positive BC cell
33 lines compared to ER α -negative ones (Fig. 1A and Supplementary Table 1).

34 To identify drugs that more likely preferentially affect ER α -positive BC cell lines, we applied
35 specific thresholds. We selected drugs with a difference in mean sensitivity between ER α -positive
36 and ER α -negative BC cell lines greater than 1 and a corresponding p-value < 0.01. By applying these
37 criteria, we compiled a list of 73 drugs (Fig. 1B and Supplementary Table 1). Notably, this list
38 included cardiac glycosides (CG) and anti-helminthic drugs, known to induce ER α degradation in BC
39 cells^{6,7,10}, as well as drugs targeting DNA polymerase or the spindle, which can induce replication
40 stress²⁰ and potentially reduce receptor expression in BC cells¹⁷. Additionally, inhibitors of the
41 ubiquitin proteasome system (UPS), known to affect ER α stability¹¹, were present in the list (Fig. 1C
42 and Supplementary Table 1).

43 A significant portion (37 drugs) of the drugs displaying increased sensitivity in ER α -positive
44 BC cell lines compared to ER α -negative ones were kinase inhibitors (Fig. 1C and Supplementary
45 Table 1). Among these, CHK1 was the most targeted kinase (8 drugs), and 1 inhibitor targeted ATR.
46 Interestingly, previous research has shown that inhibiting the ATR/CHK1 pathway induces
47

1 replication stress-dependent ER α degradation¹⁷. Additionally, a PLK1 inhibitor was also observed in
2 the list, and inhibition of PLK1 was previously reported to induce ER α degradation in BC cells^{21,22}.
3 Notably, the most represented or highest-valued kinase inhibitors in terms of mean difference
4 sensitivity among ER α -positive and ER α -negative BC cell lines or p-value were those targeting ALK
5 or AURKA and AURKB (Fig. 1D and Supplementary Table 1).

6 In light of these findings, we proceeded to examine the effects of three inhibitors of ALK
7 (namely AZD3436 – AZD, NVP-TAE684 – NVP, AP26113 – AP) and AURKA/AURKB (TAK901
8 – TAK, CCT137690 – CCT, AT9283 – AT) to determine their capacity to induce a reduction in ER α
9 levels. For screening purposes the experiments were repeated twice and generated dose-response
10 curves in seven ER α -positive BC cell lines that represent diverse clinical surrogates, histological
11 types, and variations in PR and HER2 expression (MCF-7, ZR-75-1, T47D-1, HCC1928, BT-474,
12 MDA-MB-361, and EFM192C cells) (Table 1)^{18,19}. Subsequently, we derived the effective dose 50
13 (ED₅₀) for the reduction in receptor levels, which we logarithmically transformed (-Log₂) to gauge
14 the sensitivity of each cell line to each kinase inhibitor. We then compared these sensitivity values
15 with the corresponding cell proliferation sensitivity values obtained from the DepMap portal for each
16 cell line. Utilizing linear regression analyses, we found no significant correlation between any of the
17 AURKA and AURKB inhibitors (Fig. 1E-1G and Supplementary Table 2). However, a noteworthy
18 linear correlation ($r=0.8127$; $p=0.0263$) was observed when cells were treated solely with the ALK
19 inhibitor AP (Fig. 1H-1L; Supplementary Table 2). Furthermore, we observed a linear correlation
20 ($r=0.7941$; $p=0.0329$) between the sensitivity to ER α degradation in the seven cell lines for two out
21 of three ALK inhibitors (AZD and AP) (Supplementary Fig. 1 and Supplementary Table 2). These
22 results prompted us to conduct further investigations to validate the impact of ALK on the regulation
23 of both ER α levels and cell proliferation.

24 Identification of MELK as a kinase regulating ER α stability

25 Recently, we demonstrated that the antiviral drug telaprevir (Tel) induces degradation of the
26 ER α and hampers the proliferation of several ER α -positive BC cell lines^{23,24}. Given the sensitivity
27 of ER α -positive BC cell lines to various kinase inhibitors (Fig. 1), and the fact that we previously
28 discovered that Tel inhibits the IGF1-R and AKT kinases in BC cells by reducing their intracellular
29 levels and phosphorylation status²⁴, we proceeded to conduct Affymetrix analysis on Tel-treated
30 ER α -positive BC cell lines to explore if additional kinases might be influenced by this drug and
31 potentially involved in the regulation of receptor stability. For this purpose, we decided to undertake
32 an unbiased approach by employing three different cell lines modelling the three major subtypes of
33 ER α -positive breast tumors: MCF-7 cells were chosen because they represent the LumA phenotype,
34 while BT-474 cells were selected because they belong the LumB class of BC. Finally, we also
35 performed the same experiment in a cell line modelling a metastatic BC resistant to the ET drugs
36 because they express an ER α missense mutation (i.e., Y537S) that renders the receptor hyperactive
37 and sustains uncontrolled cell proliferation^{25,26}.

38 The results revealed that Tel administration significantly reduced the mRNA levels of 21
39 kinases in MCF-7 cells, 8 in BT-474 cells, and 44 in Y537S MCF-7 cells ($FC \leq -2$; $q\text{-value} \leq 0.05$)
40 (Fig. 2A and Supplementary Table 3). Remarkably, only one kinase (CDK2) exhibited reduced levels
41 in all three cell lines, while 17 kinases (BUB1, PLK1, DCLK1, CDC7, AURKB, CDK1, PBK,
42 CAMK2D, CHK1, MELK, BUB1B, PLK4, GSG2, DYRK1B, VRK1, TTK, MASTL) were
43 commonly reduced in both MCF-7 and Y537S MCF-7 cells. Intriguingly, we found that 12 (PLK1,
44 CDC7, AURKB, CDK1, PBK, CHK1, MELK, BUB1B, PLK4, VRK1, TTK, MASTL) out of these
45 17 commonly reduced kinases (Fig. 2B and Supplementary Table 3) are part of a kinase signature
46

1 that distinguishes LumA BC from basal BC²⁷. These findings suggest that Tel reduces the levels of
2 several kinases in LumA BC cells, and this reduction may be linked to the degradation of ER α .

3 To test this hypothesis, we performed siRNA experiments using esiRNA reagents and we
4 evaluated the impact of each esiRNA treatment on ER α content in the same abovementioned seven
5 different cell lines. The experiments were repeated twice for screening purposes, and ER α levels were
6 assessed 24 hours after the administration of esiRNA. To quantify the sensitivity of each treatment
7 on ER α levels, we logarithmically transformed (-Log₂) the fold of difference in ER α levels compared
8 to controls for each esiRNA in each cell line. As shown in Fig. 2C and Supplementary Table 4,
9 treatment with esiRNA targeting the 11 kinases (PLK1, CDC7, AURKB, CDK1, PBK, MELK,
10 BUB1B, PLK4, VPK1, TTK, MASTL, excluding CHK1, as we had previously investigated its effect
11 on the regulation of ER α levels and cell proliferation in different BC cell lines¹⁷) was more effective
12 in reducing ER α levels in MCF-7, BT-474, and T47D-1 cell lines than in ZR-75-1, MDA-MB-361,
13 EFM192C, and HCC1428 cells. Notably, when we stratified the cell lines based on histological type
14 (invasive ductal carcinoma – IDC *versus* not-IDC)^{18,19}, we observed that the reduction in ER α levels
15 caused by esiRNA treatment against the 11 kinases was significantly overall higher in IDC cells
16 (MCF-7, ZR-75-1, T47D-1, BT-474) than in not-IDC cells (HCC1428, EFM192C and MDA-MB-
17 361) (Fig. 2D and Supplementary Table 4). Subsequently, we individually evaluated the effect of
18 each esiRNA treatment in IDC cells and discovered that the depletion of PLK1 and MELK resulted
19 in higher reductions in ER α levels (Fig. 2E). These findings suggest that treating IDC cell lines with
20 esiRNA targeting several kinases, which are responsible for distinguishing the LumA BC phenotype
21 from the basal BC phenotype²⁷, leads to a reduction in ER α levels. Furthermore, considering the
22 known effect of PLK1 depletion on reducing ER α levels^{21,22}, we proceeded to conduct further
23 investigations to examine the influence of MELK on the regulation of both ER α levels and cell
24 proliferation.

25 The impact of ALK and MELK in different BC subtypes

26 Subsequently, we investigated whether the effects of ALK and MELK on ER α stability were
27 specific to particular subtypes of ER α -positive BC. For this purpose, we classified the aforementioned
28 seven cell lines based on their PR and HER2 expression^{18,19}. Interestingly, the sensitivity for the
29 reduction in ER α levels of the different cell lines to the esiRNA treatment against MELK was
30 significantly higher in BC cell lines expressing PR (MCF-7, T47D-1, HCC1428, BT-474, and
31 EFM192C) (Fig. 3A, 3C and Supplementary Table 4), while the sensitivity for the reduction in ER α
32 levels of the different cell lines to AP26113 (AP)-dependent ALK inhibition was significantly higher
33 in PR-negative cells (MDA-MB-361 and ZR-75-1 cells) (Fig. 3B, 3C and Supplementary Table 4).

34 To further understand which BC phenotype could be more influenced by MELK and ALK
35 expression, we examined the public KMplotter database (<https://kmplot.com/analysis>)²⁸ to assess the
36 relapse-free survival (RFS) rate in women with ER α -positive BC, stratified based on PR and HER2
37 expression. The data revealed that women with low MELK mRNA levels displayed a significantly
38 longer RFS rate than those with high MELK mRNA levels, particularly in tumors classified as ER α -
39 positive/PR-positive/HER2-negative or ER α -positive/PR-negative/HER2-negative (Fig. 3D-3G and
40 Supplementary Table 5), with the ER α -positive/PR-positive/HER2-negative phenotype showing the
41 most significant difference. Conversely, women with low ALK mRNA levels displayed a
42 significantly longer RFS rate than those with high ALK mRNA levels only in tumors classified as
43 ER α -positive/PR-negative/HER2-positive (Fig. 3H-3M and Supplementary Table 5). These findings
44 suggest that MELK could be a potential target in ER α -positive/PR-positive/HER2-negative BC cases,
45 whereas ALK could be a target specifically in ER α -positive/PR-negative/HER2-positive tumors.
46 Remarkably, these data align with the analysis conducted in the cell lines, supporting the notion that
47

1 interference with MELK and ALK could affect ER α stability in BC cell lines stratified based on PR
2 expression. Consequently, we selected MCF-7 and MDA-MB-361 cells, which display ER α -
3 positive/PR-positive/HER2-negative and ER α -positive/PR-negative/HER2-positive phenotypes,
4 respectively, to further validate the impact of these kinases on ER α stability and BC cell proliferation.

5 6 Validation of the ALK and MELK impact on ER α levels and cell proliferation in MCF-7 and MDA- 7 MB-361 cells

8 Subsequently, we validated the impact of esiRNA-mediated depletion and inhibition of both
9 MELK and ALK on the intracellular content of ER α in MCF-7 and MDA-MB-361 cells. The results
10 demonstrate that the depletion of MELK led to a substantial reduction in ER α levels solely in MCF-
11 7 cells (Fig. 4A, 4A', and 4A''). Furthermore, treatment of MCF-7 and MDA-MB-361 cells with
12 varying concentrations of the MELK inhibitor, MELK-8a (MELKin)²⁹, for 24 hours exhibited a dose-
13 dependent decrease in ER α content in MCF-7 cells, whereas the effect on receptor levels in MDA-
14 MB-361 cells was only marginal and observed at higher doses (10 μ M) (Fig. 4B, 4B', and 4B'').
15 esiRNA-mediated depletion of ALK in both cell lines resulted in a reduction of ER α content, which
16 was significantly more pronounced in MDA-MB-361 cells compared to MCF-7 cells (Fig. 4C, 4C',
17 and 4C''). Similarly, treatment of both cell lines with different doses of the ALK inhibitor AP,
18 demonstrated a dose-dependent decrease in intracellular receptor content, with a more substantial
19 effect observed in MDA-MB-361 cells (Fig. 4D, 4D', and 4D'').

20 Subsequently, we evaluated the antiproliferative efficacy of MELKin and AP in both MCF-7
21 and MDA-MB-361 cells by generating growth curves and determining the inhibitory concentration
22 50 (IC₅₀) for each compound in each cell line. Our findings revealed that the IC₅₀ values for both cell
23 lines fell within the μ M range. Interestingly, the IC₅₀ of MELKin in MCF-7 cells was significantly
24 lower than that calculated in MDA-MB-361 cells. Conversely, the IC₅₀ of AP in MDA-MB-361 cells
25 was significantly lower than that observed in MCF-7 cells.

26 Collectively, these data indicate that interfering with MELK and ALK leads to a reduction in
27 intracellular ER α content, thereby preventing BC cell proliferation. Furthermore, our results suggest
28 that MELK predominantly controls ER α stability and cell proliferation in MCF-7 cells, while ALK
29 more strongly modulates receptor intracellular levels and cell proliferation in MDA-MB-361 cells.

30 31 The ALK- and MELK-dependent control of ER α intracellular concentration

32 Ligand-induced reduction of ER α in BC cells may result from the ligand's ability to directly
33 bind to the receptor¹⁵. To examine this, ER α binding assays were conducted using various doses of
34 AP, MELKin, and E2 to assess whether these kinase inhibitors could directly bind to ER α in vitro.
35 Only E2 (Fig. 5A) was found to displace fluorescently labeled E2, used as a tracer for purified
36 recombinant ER α , with an IC₅₀ (i.e., K_d) value of around 2.0 nM, consistent with previous reports¹⁰.
37 Next, the impact of kinase inhibition on ER α mRNA levels was investigated. Both MCF-7 and MDA-
38 MB-361 cells were treated with MELKin and AP, respectively, for 48 hours. However, no significant
39 difference in ER α mRNA content was observed in either cell line (Fig. 5B).

40 The turnover rate of ER α protein was then examined. MCF-7 and MDA-MB-361 cells were
41 treated with the protein synthesis inhibitor cycloheximide (CHX) at different time points, both in the
42 presence and absence of MELKin in MCF-7 cells and AP in MDA-MB-361 cells. As expected,
43 MELKin, AP, and CHX reduced ER α levels. However, while CHX led to a time-dependent decay of
44 the receptor, MELKin and AP effectively reduced ER α content only after 24 hours of treatment (Fig.
45 5C, 5C', 5D, and 5D'). Interestingly, both inhibitors influenced the CHX-dependent reduction in ER α
46 intracellular content after 24-hour administration (Fig. 5C, 5C', 5D, and 5D'), suggesting that the
47 kinase inhibitors can regulate ER α abundance at the post-translational level.

1 ER α stability can be modulated at the post-translational level through various cellular
2 degradative pathways, such as the 26S proteasome, lysosomes, autophagic flux, and induction of
3 replication stress^{8,17}. Therefore, we assessed the impact of each pathway on MELKin- and AP-
4 induced reduction in ER α intracellular content both in MCF-7 and in MDA-MB-361 cells. We found
5 that 24 hours administration of MELKin in MCF-7 cells and of AP in MDA-MB-361 cells determined
6 the increase in the cellular amount of LC3-II [i.e., LC3-II/(LC3-I+LC3-II)], a marker of
7 autophagosome number³⁰, thus indicating autophagosome accumulation (Fig. 5E, 5E', 5F and 5F').
8 To determine whether this increase was due to autophagic flux activation or inhibition, additional
9 experiments were conducted in the presence or absence of bafilomycin A1 (Baf), an inhibitor of the
10 fusion between autophagosomes and lysosomes³⁰. In MDA-MB-361 cells, two hours of Baf
11 administration resulted in increased LC3-II levels (Fig. 5G, 5G'), as expected³⁰. However, when Baf
12 was added in the last two hours of AP treatment, it further significantly increased the levels of LC3-
13 II compared to AP and Baf treatments alone (Fig. 5G, 5G'). Conversely, in MCF-7 cells, while two
14 hours of Baf treatment increased LC3-II content (Fig. 5H, 5H'), adding Baf in the presence of
15 MELKin did not further increase the amount of LC3-II levels induced by MELKin alone (Fig. 5H,
16 5H'). These findings indicate that AP activates autophagy in MDA-MB-361 cells, while MELKin
17 inhibits the autophagic flux at its terminal stages in MCF-7 cells.

18 Taken together, these results indicate that ALK and MELK control ER α stability through a
19 post-translational mechanism and regulate autophagy.

20 21 The impact of MELK inhibition on E2:ER α signaling to cell proliferation

22 The ER α is a ligand-activated transcription factor that regulates the expression of multiple
23 genes, both with and without the estrogen response element (ERE) sequence in their promoter regions
24 in BC cells. Full E2-induced transcriptional activation of the receptor occurs upon phosphorylation
25 of the S118 residue¹⁵. Given the strong reduction in E2 signaling observed in cell lines modelling
26 LumB BC³¹, we investigated the impact of inhibiting MELK on E2 signaling and cell proliferation
27 in MCF-7 cells. Upon E2 administration to MCF-7 cells, there was a notable increase in the
28 phosphorylation of the S118 residue (Fig. 6A, 6A', and 6A'') as expected³². Pretreatment of MCF-7
29 cells with MELKin or esiRNA-dependent depletion of MELK significantly reduced E2-induced ER α
30 S118 phosphorylation (Fig. 6A, 6A', and 6A''). To study receptor transcriptional activity, we utilized
31 MCF-7 cells stably expressing a reporter gene consisting of a promoter containing three synthetic
32 ERE sequences that control the nanoluciferase gene (NLuc) (i.e., MCF-7NLuc cells)¹³. E2 induced
33 the activation of the synthetic ERE-containing promoter, and pretreatment with MELKin in MCF-
34 7NLuc cells resulted in a dose-dependent reduction in E2-induced promoter activity (Fig. 6B).
35 Moreover, depletion of MELK (inset in Fig. 6C) prevented the E2-dependent induction of ERE-
36 containing promoter activity in MCF-7NLuc cells (Fig. 6C). As ER α controls the activation of genes
37 with or without the ERE sequence in their promoter regions¹⁵, we assessed the impact of MELK
38 inhibition on E2-dependent gene expression. Using an RT-qPCR-based array containing 89 E2-
39 sensitive genes^{7,23}, we hybridized cDNA samples generated from total RNA extracted from MCF-7
40 cells treated with E2 for 24 hours, both in the presence and absence of MELKin. As expected, most
41 of the genes included in the array were modulated by E2 (i.e., 69.7%) (Fig. 6D). Interestingly,
42 treatment with MELKin prevented the effect of E2 in 75.8% of the genes initially modulated by E2
43 in MCF-7 cells (Fig. 6D). Subsequently, we validated the effect of MELKin on some of these genes
44 in MCF-7 cells. We pre-treated MCF-7 cells with MELKin and then treated them with E2, measuring
45 the cellular levels of ERE-containing genes (presenilin 2 - pS2 and retinoic acid receptor A - RARA)
46 and those lacking the ERE sequence in their promoter region (brain-derived nerve factor - BDNF and
47 cyclin D1 - CycD1), along with the levels of ER α as an internal control. As expected, E2 induced an
48 increase in the cellular levels of pS2, RARA, BDNF, and CycD1 and led to ER α degradation after 24
49 hours of administration to MCF-7 cells (Fig. 6E-6M). Notably, inhibition of MELK, as well as

1 reduction in MELK expression, prevented the E2-induced increase in pS2, RARA, BDNF, and
2 CycD1 expression levels and resulted in an additional reduction in the receptor's intracellular content
3 (Fig. 6E-6M). Collectively, these data indicate that MELK inhibition decreases ER α transcriptional
4 activity, impedes E2's ability to activate ER α , and hinders E2-dependent gene expression.

5 Since E2-dependent activation of ER α in BC cells leads to DNA synthesis, cell cycle
6 progression, and cell proliferation¹⁵, we investigated the effect of MELK inhibition on E2's ability
7 to induce these processes in MCF-7 cells. Treatment with both MELKin and esiRNA targeting MELK
8 (inset in Fig. 7A) significantly reduced E2-induced 5-ethynyl-2'-deoxyuridine (EdU) incorporation
9 in MCF-7 cells (Fig. 7A). Furthermore, E2 increased the cell number in a time-dependent manner,
10 and co-treatment of MCF-7 cells with MELKin prevented both the basal and E2-induced time-
11 dependent increase in cell number (Fig. 7B).

12 Altogether, these findings indicate that inhibition of MELK activity interferes with E2's ability
13 to induce DNA synthesis and cell proliferation in MCF-7 cells.

14 MELK and ALK inhibitors in combination with 4OH-tamoxifen and HER2 inhibitors as a novel 15 selective treatment for specific BC subtypes

16 The obtained results suggest that MELK could serve as a promising target for treating ER α -
17 positive breast tumors with the ER α -positive/PR-positive/HER2-negative phenotype. Conversely,
18 our findings indicate that ALK could be targeted in tumors with the ER α -positive/PR-negative/HER2-
19 positive phenotype. It is worth noting that tumors with the ER α -positive/PR-positive/HER2-negative
20 phenotype are typically treated with Tam, the standard treatment for this type of tumors^{4,5}, while
21 HER2-positive tumors are treated with drugs inhibiting HER2 activity (e.g., lapatinib – Lapa,
22 erlotinib – Erlo, and gefitinib – Gef)^{4,5}. Therefore, we sought to investigate whether combining
23 MELKin with Tam and combining the ALK inhibitor AP with Lapa, Erlo, and Gef could have
24 potential benefits in MDA-MB-361 cells. Proliferation studies were performed by treating cells for
25 12 days with varying doses of MELKin together with varying doses of Tam in MCF-7 cells and
26 different doses of Lapa, Erlo, and Gef along with different doses of AP in MDA-MB-361 cells. The
27 data reveal that Tam and MELKin synergistically enhance the anti-proliferative effects of both
28 inhibitors in MCF-7 cells (Fig. 8A, 8A'). Interestingly, while AP synergistically enhances the effect
29 of all HER2 inhibitors in MDA-MB-361 cells (Fig. 8B-E), we observed that the combination of AP
30 with either Erlo or Gef was more effective than the combination of AP and Lapa in achieving an anti-
31 proliferative effect in MDA-MB-361 cells (Fig. 8B-E).

32 These findings support the concept that MELKin could be a promising candidate for
33 combinatorial treatment in ER α -positive/PR-positive/HER2-negative tumors in conjunction with
34 Tam, and the ALK inhibitor AP could be considered for combinatorial treatment in ER α -positive/PR-
35 negative/HER2-positive tumors with HER2 inhibitors.

36 Evaluation of the antiproliferative effect of MELK and ALK inhibitors in 3D models of BC

37 We finally investigated the anti-proliferative effects of MELKin and AP in MCF-7 and MDA-
38 MB-361 tumor cell spheroids and alginate-based cultures^{16,17} to assess their activity in 3D cell
39 structures³³. Both tumor spheroids and cells within alginate-based spheres demonstrated successful
40 growth within a 7-day period. Remarkably, treatment with MELKin significantly inhibited cell
41 proliferation in both MCF-7 spheroids and alginate-based structures (Fig. 9A, 9A', 9B, and 9B').
42 However, in the case of MDA-MB-361 cells, while AP administration effectively prevented
43 proliferation in alginate-based spheres, it had no significant effect on cell growth when the cells were
44 cultured as spheroids (Fig. 9A, 9A', 9B, and 9B'). These results indicate that MELKin and AP retain
45
46

1 their anti-proliferative efficacy in 3D models of BC, although they may exert their effects through
2 distinct mechanisms of action.

3 4 **Discussion**

5 The classification of breast cancer (BC) at diagnosis plays a critical role in determining the
6 pharmacological approach for treating the disease. BC classification is based on various molecular
7 and histological prognostic factors. The expression of ER α categorizes the tumor into two groups,
8 each of which can be further stratified based on the histological type of the disease and the expression
9 of PR and HER2. Additionally, PAM50 analysis of breast tumors identifies the luminal (LumA and
10 LumB) or basal origin of the disease¹⁻⁴. Notably, specific breast tumor types can be a combination
11 of all these factors, resulting in a unique tumor type for each patient, which may even be considered
12 a rare disease³⁴. The heterogeneity of BC necessitates specific drugs that can selectively target
13 particular BC subtypes to implement a personalized medicine approach. Notably, endocrine therapy
14 drugs like Tam exhibit increased sensitivity in LumA tumors compared to LumB tumors, as the latter
15 express HER2, which is better targeted by its inhibitors (erlotinib, gefitinib, lapatinib)^{4,5}.
16 Consequently, identifying drugs that can selectively target specific tumor subtypes becomes
17 increasingly important for effective BC treatment.

18 Recently, we found that certain drugs not originally intended for this purpose can induce
19 receptor degradation in ER α -positive BC cells, making them act as ‘anti-estrogen-like’ compounds
20 to prevent cell proliferation⁶⁻¹⁴. Additionally, some of these drugs selectively induced ER α
21 degradation and prevented cell proliferation only in specific BC subtypes⁶⁻¹⁴. This led us to
22 hypothesize that ER α -positive BC cells may be more sensitive to certain drugs than ER α -negative
23 BC cells due to these compounds' ability to induce ER α degradation, thereby displaying a selective
24 effect on specific BC subtypes.

25 Taking advantage of sensitivity data from over 4600 drugs tested against 26 different ER α -
26 positive and ER α -negative BC cell lines available in the DepMap portal database
27 (<https://depmap.org/portal/>), we identified a list of 73 drugs that exhibited increased sensitivity in
28 ER α -positive BC cell lines compared to ER α -negative ones. Among these drugs, we discovered 2
29 anti-helminthics compounds, 4 cardiac glycosides (CG), and 7 DNA polymerase inhibitors, known
30 to produce replication stress²⁰. Interestingly, our recent findings also demonstrated that anti-
31 helminthics clotrimazole and fenticonazole bound to ER α , induced its degradation, and prevented the
32 proliferation of ER α -positive BC cell lines⁷. Moreover, we reported that the CG compounds ouabain
33 and digoxin showed increased sensitivity in ER α -positive BC cancer cell lines compared to ER α -
34 negative BC cell lines because, in addition to inhibiting the Na/K ATPase, they hyperactivated the
35 26S proteasome, inducing receptor degradation^{6,10}. Additionally, we showed that CHK1 inhibitors
36 induced replication stress, leading to ER α degradation¹⁷. Therefore, the identified list of drugs could
37 contain molecules capable of inducing ER α degradation.

38 Remarkably, 37 out of the 73 drugs on the list are kinase inhibitors, prompting us to focus on
39 this class of molecules as kinases represent excellent drug targets controlling various pathways
40 required for cell proliferation³⁵. Most of the identified kinase inhibitors targeted CHK1 and PLK1,
41 which have been previously shown to induce receptor degradation^{17,21,22}. We also found 4 inhibitors
42 in the list for AURKA/AURKB and ALK, and their impact on BC cell proliferation was poorly
43 investigated. To address this, we studied whether the inhibition of these kinases could influence the
44 cellular amount of ER α in 7 different ER α -positive BC cell lines representing different BC molecular
45 and histological subtypes^{18,19}. We observed that ALK inhibitors led to a reduction in ER α levels.

46 We also used a hypothesis-driven approach to identify additional kinases involved in regulating
47 receptor intracellular levels by conducting Affymetrix analyses on ER α -positive BC cells treated with

1 telaprevir (Tel), an antiviral drug inducing ER α degradation by inhibiting the kinases IGF1-R and
2 AKT^{23,24}. Surprisingly, we found that Tel reduced the mRNA levels of many kinases, most of which
3 belonged to the kinase signature that distinguishes LumA BC from basal BC²⁷. We then tested the
4 impact of reducing each of these kinases on ER α levels in the aforementioned BC cell lines and found
5 that the reduction of receptor levels caused by cell treatment with esiRNA directed against these
6 kinases was predominant in invasive ductal carcinoma (IDC) cells compared to not-IDC cells.
7 Remarkably, we also observed that, in addition to PLK1, only the treatment with esiRNA directed
8 against MELK led to a reduction in ER α levels.

9 Due to the lack of information on ALK- and MELK-dependent control of ER α levels, we further
10 studied the impact of these two kinases in BC. We stratified sensitivity data for the reduction in ER α
11 levels based on the expression of PR and HER2 in ER α -positive cell lines used and observed that cell
12 lines expressing PR were more sensitive to the reduction in ER α levels induced by esiRNA directed
13 against MELK, while cells not expressing PR were more susceptible to the ALK inhibitor AP26113
14 (AP)-dependent reduction in receptor levels. Accordingly, we found that low MELK and ALK
15 mRNA expression is associated with a significantly improved patient RFS rate, depending on whether
16 the patient carries a tumor with the ER α -positive/PR-positive/HER2-negative or the ER α -
17 positive/PR-negative/HER2-positive phenotype, respectively. Thus, to investigate ALK and MELK's
18 impact, we studied MELK and ALK in ER α -positive BC cell lines showing the corresponding
19 phenotype (i.e., MCF-7 and MDA-MB-361 cells, respectively^{18,19}). Using these cell lines, we
20 demonstrated that MELK inhibition or depletion preferentially affected the control of ER α levels and
21 cell proliferation in LumA, IDC, PR-positive and HER2-negative MCF-7 cells. In this cell line,
22 interference with MELK activity or levels also prevented the receptor's ability to control E2-induced
23 transcriptional activity, gene expression, DNA synthesis, and cell proliferation. Conversely, ALK
24 inhibition or depletion selectively affected the control of ER α levels and cell proliferation in LumB,
25 adenocarcinoma, PR-negative, and HER2-positive MDA-MB-361 cells. However, we could not
26 measure the ER α signaling to cell proliferation in this cell line, as E2 has a negligible effect on LumB
27 cell lines³¹.

28 Regarding the mechanism through which ER α is degraded upon ALK and MELK inhibition,
29 we found that it occurs at post-translational level and does not imply the ability of the ALK and
30 MELK inhibitors either to directly bind to the receptor or to control the ER α mRNA levels. However,
31 we found that treatment with the MELK inhibitor blocked autophagy in MCF-7 cells, while the ALK
32 inhibitor AP induced autophagy in MDA-MB-361 cells.

33 Previous data from our lab demonstrated that autophagic flux controls basal ER α degradation,
34 and ER α is partially degraded in autophagosomes. Therefore, the effect induced by ALK and MELK
35 inhibitors on the regulation of receptor intracellular levels could occur at post-translational levels
36 through the modulation of the autophagic flux. Accordingly, in MDA-MB-361 cells, ALK inhibitor
37 AP administration induced autophagy and resulted in receptor degradation. Surprisingly, in MCF-7
38 cells, the MELK inhibitor-induced ER α degradation was accompanied by autophagic flux inhibition.
39 Two possibilities exist to explain this contradiction. ER α binds to p62^{SQSTM} and is shuttled to the
40 autophagosomes by p62^{SQSTM}³⁶. Interestingly, p62^{SQSTM} plays a critical role in the balance between
41 autophagic flux and the ubiquitin-proteasome system (UPS). Autophagy inhibition with increased
42 p62^{SQSTM} levels has been reported to deregulate p62^{SQSTM}-dependent shuttling of ubiquitinated
43 proteins to the 26S proteasome^{37,38}. Therefore, it is tempting to speculate that in MCF-7 cells treated
44 with the MELK inhibitor, ER α is degraded through the UPS via increased p62^{SQSTM}-dependent
45 shuttling to the proteasome. Additionally, in MCF-7 cells, a similar situation occurs under E2
46 administration, as E2 blocks autophagic flux and induces ER α degradation³⁶. The steady-state
47 cellular ER α content is influenced by degradative pathways acting on both neo-synthesized and

1 mature ER α fractions³⁹. We have shown that E2 impedes autophagic degradation of neo-synthesized
2 ER α without affecting autophagy's impact on the mature receptor pool³⁶. Therefore, it is also possible
3 that MELK inhibitor-induced autophagy inhibition differentially affects the neo-synthesized and
4 mature ER α pools. However, our data suggest that the autophagic control of ER α levels can follow
5 different routes in different cell lines and this differential mechanistic aspect is currently being
6 evaluated. Furthermore, our results indicate that both ALK and MELK are involved in controlling
7 autophagy. Altogether, this evidence demonstrates that MELK and ALK control ER α stability and
8 cell proliferation selectively in different BC subtypes.

9 Due to the differential effects observed in cell lines modeling various BC subtypes, we further
10 evaluated the potential use of MELK and ALK inhibitors in pre-clinical combinatorial studies with
11 drugs used to treat specific patient tumor phenotypes, including ER α -positive/PR-positive/HER2-
12 negative and ER α -positive/PR-negative/HER2-positive phenotypes. Although the MELK inhibitor
13 MELK-8a is not approved for use in humans, we observed that this drug exhibited a synergic
14 antiproliferative effect when used in combination with Tam in MCF-7 cells. On the other hand, the
15 ALK inhibitor AP, in clinical trials for patients with lung tumors⁴⁰, showed synergy with HER2
16 inhibitors, with varying effectiveness when co-administered with gefitinib and erlotinib compared to
17 lapatinib. These results demonstrate that MELK inhibition could be a valuable strategy for treating
18 BC patients with the ER α -positive/PR-positive/HER2-negative phenotype, while ALK inhibition, in
19 combination with specific HER2 inhibitors, could be effective for treating ER α -positive/PR-
20 negative/HER2-positive BC patients. Finally, the use of MELK and ALK inhibitors in BC patients is
21 further supported by the fact that these inhibitors retained their anti-proliferative activities, albeit with
22 some differences, in 3D models of BC, which mimic a context closer to the tumor environment³³.

23 **Conclusions**

24 In this study, we present new findings identifying MELK and ALK as promising targets for the
25 treatment of ER α -positive BC. Notably, we have uncovered that distinct BC subtypes, namely ER α -
26 positive/PR-positive/HER2-negative and ER α -positive/PR-negative/HER2-positive, exhibit
27 selective sensitivity to the inhibition of these kinases, respectively. Our research further demonstrates
28 that targeting ER α -positive cells with the ER α -positive/PR-positive/HER2-negative receptor profile
29 using the MELK inhibitor alone or in combination with the endocrine therapy drug Tam, as well as
30 targeting ER α -positive cells representing the ER α -positive/PR-negative/HER2-positive phenotype
31 with the ALK inhibitor AP alone or in combination with HER2 activity-blocking drugs such as
32 gefitinib and erlotinib, offer promising strategies to curb the cell proliferation of specific ER α -positive
33 BC subtypes.

34 Consequently, we propose that the targeted inhibition of MELK and ALK using small
35 molecules could hold significant potential for personalized BC management. These findings may
36 pave the way for more effective and tailored treatments for individuals with ER α -positive BC,
37 offering new avenues for precision medicine in this context.

38 **Methods**

39 *Cell Culture and Reagents*

40 The following cell lines and chemicals were used: MCF-7, T47D-1, ZR-75-1, HCC1428, BT-474,
41 and MDA-MB-361 cell lines were obtained from ATCC (USA), while EFM192C cells were obtained
42 from DSMZ (Braunschweig, Germany). All cell lines were maintained according to the
43 manufacturer's instructions. The following reagents and antibodies were used: 17 β -estradiol (E2),
44 DMEM (with and without phenol red), and fetal calf serum were purchased from Sigma-Aldrich (St.
45 Louis, MO). The Bradford protein assay kit, anti-mouse, and anti-rabbit secondary antibodies were
46 obtained from Bio-Rad (Hercules, CA). Antibodies against ER α (F-10, mouse), pS2 (FL-84, rabbit),
47
48

1 cyclin D1 (H-295 rabbit), ALK (F-12, mouse), and RARA (C-1, mouse) were obtained from Santa
2 Cruz Biotechnology (Santa Cruz, CA, USA). Additionally, anti-MELK (ab273015, rabbit) and anti-
3 BDNF (ab108319, rabbit) antibodies were purchased from Abcam (Cambridge, UK). Anti-phospho
4 ER α (Ser118, mouse) antibody was obtained from Cell Signaling, and anti-vinculin (mouse) and anti-
5 LC3 (mouse) antibodies were purchased from Sigma-Aldrich (St. Louis, MO, USA).
6 Chemiluminescence reagent for Western blot was obtained from BioRad Laboratories (Hercules, CA,
7 USA). For specific experiments, the following compounds were used: 4OH-Tamoxifen,
8 cycloheximide (CHX), and esiRNA library were purchased from Sigma-Aldrich (St. Louis, MO,
9 USA). MELK-8a hydrochloride, TAK-901, AT-9283, CCT-137690, AP26113, NVP-TAE-684,
10 AZD-3463, Lapatinib, Gefitinib, and Erlotinib were purchased from Selleck Chemicals (USA). The
11 PolarScreen™ ER α Competitor Assay Kit, Green (A15882) was acquired from Thermo Scientific.
12 All other products used were from Sigma-Aldrich, and analytical- or reagent-grade products were
13 used without further purification. To verify the authenticity of the cell lines, STR analysis was
14 performed by BMR Genomics (Italy).

15

16 *In Vitro ER α Binding Assay*

17 The in vitro ER α binding assay employed a fluorescence polarization (FP) method to assess the
18 binding affinity of MELK-8a hydrochloride, AP26113, and 17 β -estradiol (E2) with recombinant
19 ER α . The FP assay was conducted using the PolarScreen™ ER α Competitor Assay Kit, Green
20 (A15882, Thermo Scientific), following established procedures described in ¹⁷.

21 *Measurement of ER α Transcriptional Activity*

22 The ER α transcriptional activity was assessed by measuring the expression of nanoluciferase
23 (NLuc)-PEST, a reporter gene containing an estrogen response element (ERE), in stably transfected
24 MCF-7 cells. After 24 hours of compound administration, the NLuc-PEST expression was
25 determined following the described procedure ^{13,41}.

26

27 *Cell Manipulation for Western Blot Analyses*

28 Cells were initially cultured in DMEM containing phenol red and 10% fetal calf serum for 24
29 hours. Subsequently, the cells were treated with various compounds at specified doses and time
30 periods as indicated. Before E2 stimulation, cells were cultured in DMEM without phenol red and
31 10% charcoal-stripped fetal calf serum for 24 hours. Addition of MELK8a occurred 24 hours prior to
32 E2 administration. Following the treatments, cells were lysed in Yoss Yarden (YY) buffer, which
33 consisted of 50 mM Hepes (pH 7.5), 10% glycerol, 150 mM NaCl, 1% Triton X-100, 1 mM EDTA,
34 and 1 mM EGTA, supplemented with protease and phosphatase inhibitors. For Western blot analysis,
35 20–30 μ g of protein was loaded onto SDS-gels. Gels were run, and the proteins were transferred to
36 nitrocellulose membranes using a Turbo-Blot semidry transfer apparatus from Bio-Rad (Hercules,
37 CA, USA). Immunoblotting was performed by incubating the membranes with 5% milk or bovine
38 serum albumin for 60 minutes, followed by overnight incubation with the designated antibodies.
39 Subsequently, secondary antibody incubation was carried out for an additional 60 minutes. Finally,
40 the protein bands were detected using a Chemidoc apparatus from Bio-Rad (Hercules, CA, USA).

41

42 *Small Interference RNA*

43 For the small interference RNA (siRNA) experiments, cells were transfected with esiRNA
44 targeting the specific proteins of interest. The transfection procedure was conducted using
45 Lipofectamine RNAi Max (Thermo Fisher), following established protocols described in ⁴².

46

47 *Cell Proliferation and 3D Cell Culture Assays*

48 The xCELLigence DP system (ACEA Biosciences, Inc., San Diego, CA) Multi-E-Plate station
49 was utilized to measure the time-dependent response to the specified drugs by real-time cell analysis
50 (RTCA), following previously reported protocols ^{10,13,17,23}. Synergy studies were conducted using

1 Crystal Violet staining, as described in⁴³. The synergy was subsequently calculated using Combenefit
2 freeware software¹⁷. Alginate-based and tumor spheroid cultures were carried out following
3 established procedures as previously reported¹⁷.

4 *RNA isolation and qPCR analysis.*

5 Gene-specific forward and reverse primers were designed using the OligoPerfect Designer
6 software program (Invitrogen, Carlsbad, CA, USA). For human ER α , the primers used were 5'-
7 GTGCCTGGCTAGAGATCCTG-3' (forward) and 5'-AGAGACTTCAGGGTGCTGGA-3'
8 (reverse). For human GAPDH, the primers used were 5'-CGAGATCCCTCCAAAATCAA-3'
9 (forward) and 5'-TGTGGTCATGAGTCCTTCCA-3' (reverse). Total RNA was extracted from the
10 cells using TRIzol Reagent (Invitrogen, Carlsbad, CA, USA), following the manufacturer's
11 instructions. For gene expression analysis, cDNA synthesis and qPCR were performed using the
12 GoTaq 2-step RT-qPCR system (Promega, Madison, MA, USA) with an ABI Prism 7900HT
13 Sequence Detection System (Applied Biosystems, Foster City, CA, USA), according to the
14 manufacturer's instructions. Each sample was tested in triplicates, and the experiment was repeated
15 twice to ensure accuracy and reproducibility. Gene expression levels were normalized to GAPDH
16 mRNA levels as an internal control.

17 *Gene Arrays Analyses*

18 Gene Arrays Analyses were conducted as follows: Total RNA was extracted from cells using
19 TRIzol reagent (Invitrogen, Carlsbad, CA, USA) following the manufacturer's guidelines. For gene
20 expression analysis, the GoTaq 2-step RT-qPCR system (Promega, Madison, MA, USA) was utilized
21 to perform cDNA synthesis and qPCR. The ABI Prism 7900 HT Sequence Detection System (Applied
22 Biosystems, Foster City, CA, USA) was used for qPCR analysis, following the manufacturer's
23 instructions. To analyze ER α target gene expression, the PrimePCR Estrogen receptor signaling (SAB
24 Target List) H96 panel (Bio-Rad Laboratories, Hercules, CA, USA) was employed for RT-qPCR-
25 based gene array analysis, as per the manufacturer's instructions. Gene expression data were
26 normalized to the levels of GAPDH mRNA present in the array. Genes were considered affected if
27 their fold induction was above 1.5 or below 0.7 compared to the control sample.

28 *Affymetrix analysis.*

29 Total RNA was extracted using RNeasy kit (Qiagen), according to manufacturer's protocol,
30 and was quantified using a NanoDrop 2000 system (Thermo Scientific). A GeneChip Pico Reagent
31 Kit (Affymetrix) was used to amplify 5 ng of total RNA, according to the manufacturer's protocol.
32 Quality control of the RNA samples was performed using an Agilent Bioanalyzer 2100 system
33 (Agilent Technologies). Gene expression profiling was performed using the Affymetrix GeneChip®
34 Human Clariom S Array (Thermo Fisher Scientific), including more than 210,000 distinct probes
35 representative of 21,448 annotated genes (Genome Reference Consortium Human Build 38
36 (GRCh38); https://www.ncbi.nlm.nih.gov/datasets/genome/GCF_000001405.26/). RNA samples
37 were amplified, fragmented, and labeled for array hybridization according to manufacturer's
38 instruction. Samples were then hybridized overnight, washed, stained, and scanned using the
39 Affymetrix GeneChip Hybridization Oven 640, Fluidic Station 450 and Scanner 3000 7G (Thermo
40 Fisher Scientific), to generate raw data files (.CEL files). Quality control and normalization of
41 Affymetrix .CEL files were performed using the TAC software (v4.0; Thermo Fisher Scientific), by
42 performing the "Gene level SST-RMA" summarization method with human genome version hg38
43 (https://www.ncbi.nlm.nih.gov/assembly/GCF_000001405.26/). Gene expression data were log₂
44 transformed before analyses. Class comparison analysis for identifying differentially regulated genes
45
46
47

1 was performed using TAC software by selecting a fold-change (FC) of ≥ 2 and FDR adjusted p-value
2 (Benjamini-Hochberg Step-Up FDR-controlling Procedure) ≤ 0.05 as cutoff.

3

4 *5-ethynyl-2'-deoxyuridine (EdU) Incorporation Assay*

5 The cell medium was supplemented with 5-ethynyl-2'-deoxyuridine (EdU) during the last 30
6 minutes of cell growth. After the EdU incubation, the cells were fixed and permeabilized. The EdU
7 assay was performed using the Click-iT™ EdU Cell Proliferation Kit for Imaging, Alexa Fluor™ 488
8 dye, following the manufacturer's instructions. Fluorescence was measured directly in 96-well plates,
9 with each sample being repeated at least in triplicate. The measurements were performed using a
10 Tecan Spark Reader.

11

12 *Statistical Analysis*

13 Statistical analysis was conducted using InStat version 8 software system (GraphPad Software
14 Inc., San Diego, CA). Densitometric analyses were carried out using Image J freeware software,
15 where the band intensity of the protein of interest was quantified relative to the loading control band
16 (vinculin) intensity. The p-values and the specific statistical test used (either Student t-test or ANOVA
17 Test) are provided in the figure captions.

18

19 **List of Abbreviations**

20 **AI:** Aromatase inhibitors

21 **AKT:** V-Akt Murine Thymoma Viral Oncogene Homolog 1

22 **ALK:** Anaplastic lymphoma kinase

23 **AP:** AP26113

24 **ATR:** Ataxia Telangiectasia And Rad3-Related Protein

25 **AURKA:** Aurora kinase A

26 **AURKB:** Aurora kinase B

27 **Baf:** Bafilomycin A1

28 **BC:** breast cancer

29 **BDNF:** Brain Derived Neurotrophic Factor

30 **BRCA1:** Breast cancer type 1 susceptibility protein

31 **BUB1:** Mitotic Checkpoint Serine/Threonine-Protein Kinase BUB1

32 **BUB1B:** BUB1 Mitotic Checkpoint Serine/Threonine Kinase B

33 **CAMK2D:** Calcium/Calmodulin Dependent Protein Kinase II Delta

34 **CDC7:** Cell Division Cycle 7

35 **CDK1:** cyclin-dependent kinase 1

36 **CDK2:** cyclin-dependent kinase 2

37 **CHK1:** Checkpoint Kinase 1

38 **CHX:** Cycloheximide

39 **CycD1:** cyclin D1

40 **DCLK1:** Doublecortin Like Kinase 1

41 **DMEM:** Dulbecco's Modified Eagle Medium

42 **DYRK1B:** Dual Specificity Tyrosine Phosphorylation Regulated Kinase 1B

43 **E2:** 17 β -estradiol

44 **EC50:** Effective concentration 50

45 **EdU:** 5-ethynyl-2'-deoxyuridine

46 **ERE:** estrogen responsive element

47 **Erlo:** Erlotinib

48 **ER α :** estrogen receptor α

49 **ET:** Endocrine therapy

50 **FDA:** Food and Drug Administration

1 **FOXA1:** Forkhead Box A1
2 **GART:** Phosphoribosylglycinamide Formyltransferase, Phosphoribosylglycinamide Synthetase,
3 Phosphoribosylaminoimidazole Synthetase
4 **Gef:** Gefitinib
5 **GSG2:** Histone H3 Associated Protein Kinase
6 **HER2:** Human Epidermal Growth Factor Receptor 2
7 **IC50:** Inhibitory concentration 50
8 **IDC:** Invasive ductal carcinoma
9 **IGF-1R:** Insulin-like growth factor 1 receptor
10 **Kd:** Dissociation constant
11 **Lapa:** Lapatinib
12 **LumA:** Luminal A
13 **LumB:** Luminal B
14 **MASTL:** Microtubule Associated Serine/Threonine Kinase Like
15 **MBC:** Metastatic breast cancer
16 **MELK:** Maternal Embryonic Leucine Zipper Kinase
17 **MELKin:** MELK-8a – MELK inhibitor
18 **mRNA:** Messenger ribonucleic acid
19 **NLuc:** Nanoluciferase
20 **p62^{SQSTM}:** protein 62/sequestrosome
21 **PBK:** PDZ Binding Kinase
22 **PLK:** Polo-like kinase
23 **PLK4:** Polo-like kinase 4
24 **PR:** Progesterone Receptor
25 **pS2:** presenelin2
26 **RARA:** retinoic acid receptor alpha
27 **RFS:** relapse free survival
28 **Tam:** 4OH-tamoxifen
29 **Tel:** Telaprevir
30 **TTK:** Phosphotyrosine Picked Threonine-Protein Kinase
31 **UPS:** Ubiquitin proteasome system
32 **VRK1:** VRK Serine/Threonine Kinase 1
33 **YY:** Buffer: Yoss Yarden Buffer

34 35 **Acknowledgements**

36 The research leading to these results has received funding from AIRC under IG 2018 - ID. 21325
37 project – P.I. Acconcia Filippo. This study was also supported by grants from Ateneo Roma Tre to
38 FA. The Grant of Excellence Departments 2023-2027, MIUR (ARTICOLO 1, COMMI 314 – 337
39 LEGGE 232/2016) to the Department of Science, University Roma TRE is also gratefully
40 acknowledged. The authors are grateful to Prof. Simak Ali, University of London Imperial College
41 for the gift of the MCF-7 Y537S cells.

42 43 **Authors' contributions**

44 SB performed all the experiments regarding MELK and some regarding ALK. SP performed almost
45 all the experiments regarding ALK. FB performed Affymetrix analyses. MC performed experiments
46 in 3D model system of breast cancer cells. FA performed the in-silico evaluations, analyzed the data,
47 conceived the experiments, wrote the paper. All authors, which contributed to manuscript revision
48 and editing, read and approved the final manuscript.

49 50 **Data availability Statement**

1 All the original Western blots with replicates of the experiments are available as a separate file
2 uploaded together with this work. All the Kaplan-Meier curves were retrieved by the Kaplan-Meier
3 Plotter database and given in supplementary table 5 as downloaded by the website
4 (<https://kmplot.com/analysis/>)²⁸. All the datasets used to generate figure 1 were downloaded by the
5 Broad Institute through the DepMap portal (<https://depmap.org/portal>) and are available in
6 supplementary table 1 and table 2. Datasets used to generate figure 2A and 2B are given in
7 supplementary table 3. Data used to generate figure 2C, 2D and 2E are given in supplementary table
8 4. The results of the esiRNA and the three ALK, AURKA/AURKB inhibitor screenings in the seven
9 breast cancer cell lines for measuring the ER α levels as well as those for growth curve analyses, which
10 were produced and analyzed during the current study, are available from the corresponding author
11 upon reasonable request.

12
13 Competing interests: The authors declare that they have no competing interests.

14 15 **Figure Captions.**

16 **Figure 1. Potential Regulation of ER α Stability by ALK Kinase.**

17 (A) Volcano plot illustrating differences in drug sensitivity between ER α -positive and ER α -negative
18 breast cancer (BC) cell lines. Data sourced from the DepMap portal (<https://depmap.org/portal>). Each
19 dot represents a drug's value in the database. (B) Volcano plot revealing differences in drug sensitivity
20 between ER α -positive and ER α -negative BC cell lines, after applying the specified thresholds (please
21 see the text) for positive hit selection. Each dot represents a drug's value in the database, and color
22 dots correspond to drugs highlighted in panels C and D. (C) Number of compounds identified as
23 positive hits in panel (B), categorized as indicated alongside panel C. (D) Number of kinase inhibitors
24 identified as positive hits in panel (C), with the target of each kinase inhibitor specified alongside
25 panel D. (E-F) Linear regression and Spearman Correlation values between the sensitivity to
26 AURKA/AURKB inhibitors TAK901 – TAK (E), CCT137690 – CCT (F), AT9283 – AT (G), or to
27 ALK inhibitors AZD3436 – AZD (H), NVP-TAE684 – NVP (I), and AP26113 – AP (L), as
28 downloaded from the DepMap portal (<https://depmap.org/portal>), and the effective concentration 50
29 (EC₅₀) for inhibitor-induced reduction in ER α intracellular levels in corresponding BC cell lines.
30 Main panels display the correlation coefficient (r) and p-values.

31 32 **Figure 2. Potential Involvement of MELK Kinase in Regulating ER α Stability.**

33 (A) Venn diagram illustrating the number of modulated kinases (FC \leq -2; q-value \leq 0.05) as obtained
34 through Affymetrix analyses in MCF-7, BT-474, and Y537S MCF-7 cells following a 24-hour
35 administration of telaprevir (Tel - 20 μ M). (B) Venn diagram displaying the kinases commonly
36 modulated in MCF-7 and Y537S MCF-7 cells, along with the kinase signature identified in²⁷. (C)
37 Sensitivity values in the indicated cell lines, reflecting the reduction in ER α intracellular levels
38 assessed after treatment with esiRNA targeting the specific kinases identified in panel (B); each dot
39 represents the value of a specific esiRNA. (D) Sensitivity values for reduction in ER α intracellular
40 levels evaluated after treatment with esiRNA targeting the specific kinases identified in panel (B),
41 stratified based on the histological type (invasive ductal carcinoma – IDC versus not-IDC) of the
42 breast cancer (BC) cell lines used; each dot represents the value of a specific esiRNA. Statistical
43 significance is indicated by *** (p<0.001) calculated using the Student-t test. (E) Sensitivity values
44 for reduction in ER α intracellular levels assessed after treatment with esiRNA targeting the indicated
45 kinases in IDC BC cell lines; each dot represents the value of the indicated esiRNA in the specific
46 IDC cell line. For further details, please refer to the main text.

47 48 **Figure 3. Breast Cancer Subtype Sensitivity to ALK and MELK Inhibition.**

49 (A) Sensitivity values in the indicated cell lines representing different breast cancer (BC) subtypes
50 for reduction in ER α intracellular levels evaluated after treatment with esiRNA targeting MELK (A)
51 or after administration of different doses of AP26113 – AP (B) and (C) stratified based on

1 progesterone receptor (PR) expression. Statistical significance is indicated by * ($p < 0.05$) calculated
2 using the Student-t test. Kaplan-Meier plots showing the relapse-free survival (RFS) probability in
3 women with breast tumors expressing different levels of ER α , progesterone receptor (PR), and HER2
4 in relation to MELK mRNA levels (D-G) or ALK mRNA levels (H-M). The p-values for significant
5 differences between RFS are provided in each panel. Data obtained from the website
6 (<https://kmplot.com/analysis/>). All possible cutoff values between the lower and upper quartiles are
7 automatically computed (i.e., auto-select best cutoff on the website), and the best-performing
8 threshold is used as a cutoff²⁸.

9 10 **Figure 4. Confirmation of ALK and MELK Inhibition Effects on ER α Levels and Cell** 11 **Proliferation in MCF-7 and MDA-MB-361 Cell Lines.**

12 Western blot analyses of ER α expression levels in MCF-7 and MDA-MB-361 cells treated with either
13 MELK esiRNA (A, A') or ALK esiRNA oligonucleotides for 24 hours (C, C'), as well as with
14 indicated doses of the MELK inhibitor MELK-8a (MELKin) (B, B') or the ALK inhibitor AP26113
15 (AP) (D, D') for 48 hours. Representative blot images are shown. (A'', B'', C'', and D'')
16 Densitometric analyses of the corresponding blots. In panels A'' and C'', significant differences were
17 calculated using the ANOVA test, and * indicates differences compared to control (CTR) samples
18 (** $p < 0.01$, **** $p < 0.0001$), while ° indicates differences compared to esiRNA-treated samples
19 (° $p < 0.01$). In panels B'' and D'', significant differences were calculated for each dose in the different
20 cell lines using the Student-t test, and * represents a p-value < 0.05 , *** represents p-values < 0.001 ,
21 and **** represents p-values < 0.0001 . (E) The inhibitor concentration 50 (IC₅₀) calculated for both
22 MCF-7 and MDA-MB-361 cells treated with different doses of the MELK inhibitor MELK8a
23 (MELKin) for 7 days. Each dot represents an experimental replica. Significant differences were
24 calculated using the Student-t test, and **** indicates a p-value < 0.0001 . (F) The inhibitor
25 concentration 50 (IC₅₀) calculated for both MCF-7 and MDA-MB-361 cells treated with different
26 doses of the ALK inhibitor AP26113 (AP) for 7 days. Each dot represents an experimental replica.
27 Significant differences were calculated using the Student-t test, and * indicates a p-value < 0.05 .

28 29 **Figure 5. Mechanism of MELK and ALK Regulation on ER α Intracellular Levels in MCF-7** 30 **and MDA-MB-361 Cells.**

31 (A) In vitro ER α competitive binding assays were performed for the MELK inhibitor MELK-8a
32 (MELKin), the ALK inhibitor AP26113 (AP), and 17 β -estradiol (E2) at different compound doses,
33 using fluorescent E2 as the tracer. The graph shows the relative inhibitor concentration 50 (IC₅₀, i.e.,
34 K_d) values. The experiment was conducted twice with five replicates. (B) Real-time qPCR analysis
35 of ER α mRNA levels in MCF-7 cells treated for 24 hours with the MELK inhibitor MELK-8a
36 (MELKin, and in MDA-MB-361 cells treated for 48 hours with the ALK inhibitor AP26113 (AP-
37 1 μ M). The experiment was repeated twice with three replicates, and each dot represents an
38 experimental replica. Western blot and relative densitometric analysis of ER α levels in MCF-7 cells
39 (C) and in MDA-MB-361 cells (D) treated with cycloheximide (CHX - 1 μ M and 0.5 μ M, respectively)
40 at different time points, both in the presence and absence of the MELK inhibitor MELK-8a (MELKin
41 - 10 μ M) and the ALK inhibitor AP26113 (AP - 1 μ M). Representative blot images are shown.
42 Significant differences with respect to the control (CTR) samples are calculated using the Student t-
43 test and indicated by **** ($p < 0.0001$). Significant differences with respect to the CHX or inhibitor
44 samples are calculated using the Student t-test and indicated by ° and # ($p < 0.05$), respectively.
45 Western blot analysis and relative densitometric analyses of LC3 cellular levels in MCF-7 cells
46 treated with the MELK inhibitor MELK-8a (MELKin - 10 μ M) (E, E') and in MDA-MB-361 cells
47 treated with the ALK inhibitor AP26113 (AP - 1 μ M) (F, F') for 24 hours, both in the presence and
48 absence of bafilomycin A1 (Baf - 100 nM) administration in the last 2 hours of treatment (G, G', H,
49 and H'). LC3 quantitation was performed using the formula LC3-II/(LC3-I+LC3-II). Representative
50 blot images are shown. Significant differences with respect to the control (CTR) samples are

1 calculated using the ANOVA test and indicated by **** (p < 0.0001). Significant differences with
2 respect to the Baf samples are calculated using the ANOVA test and indicated by °°°° (p < 0.0001).

3 4 **Figure 6. MELK Inhibition Impacts E2:ER α Transcription Signaling in MCF-7 Cells.**

5 (A) Western blot and relative densitometric analyses of ER α and ER α S118 phosphorylation
6 expression levels in MCF-7 cells pre-treated with the MELK inhibitor MELK-8a (MELKin - 10 μ M)
7 for 24 hours (A, A'') or with MELK esiRNA (A' and A'') and then treated for 30 minutes with 17 β -
8 estradiol (E2 - 1 nM). Representative blot images are shown. Significant differences with respect to
9 the untreated (-) sample are calculated using the ANOVA test and indicated by **** (p-value <
10 0.0001). Significant differences with respect to the E2-treated sample are calculated using the
11 ANOVA test and indicated by °°° (p-value < 0.001) or °°°° (p-value < 0.0001). (B) Estrogen response
12 element promoter activity in MCF-7 ERE-NLuc cells pre-treated with the MELK inhibitor MELK-
13 8a (MELKin - 10 μ M) for 24 hours (B) or with MELK esiRNA (C) and then treated with 17 β -estradiol
14 (E2 - 1 nM) for an additional 24 hours. The experiments were performed three times in quintuplicate.
15 Significant differences were calculated using the ANOVA test. ** (p-value < 0.01) and **** (p-value
16 < 0.0001) indicate significant differences with respect to the untreated (-) sample. ° (p-value < 0.05)
17 and °°°° (p-value < 0.0001) indicate significant differences with respect to the E2-treated sample.
18 ##### (p-value < 0.0001) indicates significant differences with respect to the MELK esiRNA-treated
19 sample. (C) Pie diagrams illustrating the percentages of modulated array genes in MCF-7 cells pre-
20 treated with the MELK inhibitor MELK-8a (MELKin - 10 μ M) for 24 hours and then treated with
21 17 β -estradiol (E2 - 1 nM) for an additional 24 hours. Percentages and categories of genes are
22 indicated. (D) Western blot of presenilin 2 (pS2), retinoic acid receptor A (RARA), brain-derived
23 nerve factor (BDNF), cyclin D1 (CycD1), and ER α expression levels in MCF-7 cells pre-treated with
24 the MELK inhibitor MELK-8a (MELKin - 10 μ M) for 24 hours (E) or with MELK esiRNA (F) and
25 then treated with 17 β -estradiol (E2 - 1 nM) for an additional 24 hours. Representative blot images are
26 shown. Densitometric and statistical analyses are reported for each protein in panels F-M. Significant
27 differences were calculated using the ANOVA test. **, *** and **** indicate significant differences
28 with respect to the untreated (-) sample. °, °°, °°° and °°°° (p-value < 0.05, < 0.01, 0.001 and < 0.0001,
29 respectively) indicate significant differences with respect to the E2-treated sample. ### (p-value <
30 0.001) indicates significant differences with respect to the MELKin or MELK esiRNA-treated
31 samples. Each dot represent an experimental replica.

32 33 **Figure 7. Impact of MELK Inhibition on E2-Induced Cell Proliferation in MCF-7 Cells.**

34 (A) 5-ethynyl-2'-deoxyuridine (EdU) incorporation assay in MCF-7 cells treated with 17 β -estradiol
35 (E2 - 1 nM) for 24 hours after 24 hours pre-treatment with the MELK inhibitor MELK-8a (MELKin
36 - 10 μ M) or with MELK esiRNA. The experiments were performed twice in quintuplicate. Significant
37 differences were calculated using the ANOVA test. **** (p-value < 0.0001) indicates significant
38 differences with respect to the untreated (-) sample. °°°° (p-value < 0.0001) indicates significant
39 differences with respect to the E2-treated sample. (B) The graphs show the normalized cell index
40 (i.e., cell number) detected with the xCelligence DP device and calculated at each time point with
41 respect to the control sample. Each sample was measured in quadruplicate. MCF-7 cells were treated
42 with 17 β -estradiol (E2 - 1 nM) and the MELK inhibitor MELK-8a (MELKin - 10 μ M) when cells
43 were plated. Dotted lines represent standard deviations.

44 45 **Figure 8. Synergy between MELK and 4OH-Tamoxifen in MCF-7, and between ALK and 46 HER2 Inhibitors in MDA-MB-361 Cells.**

47 (A) Synergy map of 12-day-treated MCF-7 cells with different doses of 4OH-Tamoxifen (Tam) and
48 the MELK inhibitor MELK-8a (MELKin). (B') Growth curves in MCF-7 cells showing the
49 synergistic effect of each combination of compounds with selected doses. Significant differences
50 were calculated using the ANOVA test. **** (p-value < 0.0001) indicates significant differences with
51 respect to the untreated (i.e., -,-) sample. °°°° (p-value < 0.0001) indicates significant differences with

1 respect to Tam treated sample. ^^^^ (p-value < 0.0001) indicates significant differences with respect
 2 to MELKin treated sample. Synergy map of 12-day-treated MDA-MB-361 cells with different doses
 3 of the ALK inhibitor AP26113 (AP) and the HER2 inhibitors erlotinib (Erlo) (B), gefitinib (Gef) (C),
 4 and lapatinib (Lapa) (D). (E) Growth curves in MDA-MB-361 cells showing the synergistic effect of
 5 each combination of compounds with selected doses. Significant differences were calculated using
 6 the ANOVA test. *** (p-value < 0.001) indicates significant differences with respect to the untreated
 7 (i.e., -,-) sample. °°, °°°° (p-value < 0.001 and < 0.0001, respectively) indicates significant
 8 differences with respect to Erlo, Gef, and Lapa treated samples. ^ (p-value < 0.05) indicates
 9 significant differences with respect to AP treated sample.

10 **Figure 9. Effect of MELK and ALK Inhibitors in 3D Models of Breast Cancer.**

11 Images (A, B) and quantitation (A', B') of tumor spheroids' surface area (B, B') and alginate-based
 12 cultures (A, A') generated in MCF-7 and MDA-MB-361 cells, treated at time 0 with the MELK
 13 inhibitor MELK-8a (MELKin - 10µM), the ALK inhibitor AP26113 (AP - 1µM), or left untreated
 14 (CTR) for 7 days. The number of replicates is represented by solid dots in the graphs. Significant
 15 differences with respect to the CTR sample were determined using unpaired two-tailed ANOVA test:
 16 **** (p-value < 0.0001); ** (p-value < 0.01). Scale bars equal to 50.0 µm.

17 **Tables**

<i>Cells</i>	<i>ERα</i>	<i>PR</i>	<i>HER2</i>	<i>Histotype</i>	<i>PAM50</i>
<i>MCF-7</i>	+	+	-	IDC	LumA
<i>T47D-1</i>	+	+	-	IDC	LumA
<i>ZR-75-1</i>	+	-	-	IDC	LumA
<i>HCC1428</i>	+	+	-	Adenocarcinoma	LumA
<i>BT-474</i>	+	+	+	IDC	LumB
<i>MDAMB361</i>	+	-	+	Adenocarcinoma	LumB
<i>EFM192C</i>	+	+	+	Adenocarcinoma	LumB

18
 19
 20
 21 **Table 1: Different classification of the breast cancer cell lines used.** ERα: estrogen receptor α; PR:
 22 progesterone receptor; HER2: Human Epidermal Growth Factor Receptor 2; IDC: invasive ductal
 23 carcinoma; LumA: luminal A; LumB: luminal B.

24 **References**

- 25
 26 1 Morganti, S. C., G. Moving beyond endocrine therapy for luminal metastatic breast cancer in
 27 the precision medicine era: looking for new targets. *EXPERT REVIEW OF PRECISION*
 28 *MEDICINE AND DRUG DEVELOPMENT*, doi:10.1080/23808993.2020.1720508 (2020).
 29 2 Parsons, J. & Francavilla, C. 'Omics Approaches to Explore the Breast Cancer Landscape.
 30 *Front Cell Dev Biol* **7**, 395, doi:10.3389/fcell.2019.00395 (2019).
 31 3 Johansson, H. J. *et al.* Breast cancer quantitative proteome and proteogenomic landscape.
 32 *Nature communications* **10**, 1600, doi:10.1038/s41467-019-09018-y (2019).
 33 4 Tsang, J. Y. S. & Tse, G. M. Molecular Classification of Breast Cancer. *Adv Anat Pathol* **27**,
 34 27-35, doi:10.1097/PAP.000000000000232 (2020).
 35 5 Lumachi, F. *et al.* Endocrine therapy of breast cancer. *Curr Med Chem* **18**, 513-522, doi:not
 36 available. PMID: 21143113. (2011).
 37 6 Acconcia, F. Evaluation of the Sensitivity of Breast Cancer Cell Lines to Cardiac Glycosides
 38 Unveils ATP1B3 as a Possible Biomarker for the Personalized Treatment of ERα
 39 Expressing Breast Cancers. *International journal of molecular sciences* **23**,
 40 doi:10.3390/ijms231911102 (2022).
 41 7 Cipolletti, M. *et al.* A new anti-estrogen discovery platform identifies FDA-approved
 42 imidazole anti-fungal drugs as bioactive compounds against ERα expressing breast cancer
 43 cells. *International journal of molecular sciences* **22**, doi:10.3390/ijms22062915 (2021).

- 1 8 Busonero, C., Leone, S., Bartoloni, S. & Acconcia, F. Strategies to degrade estrogen receptor
2 alpha in primary and ESR1 mutant-expressing metastatic breast cancer. *Mol Cell Endocrinol*
3 **480**, 107-121, doi:10.1016/j.mce.2018.10.020 (2019).
- 4 9 Busonero, C., Leone, S. & Acconcia, F. Emetine induces estrogen receptor alpha degradation
5 and prevents 17beta-estradiol-induced breast cancer cell proliferation. *Cellular oncology*,
6 doi:10.1007/s13402-017-0322-z (2017).
- 7 10 Busonero, C. *et al.* Ouabain and Digoxin Activate the Proteasome and the Degradation of the
8 ER α in Cells Modeling Primary and Metastatic Breast Cancer. *Cancers (Basel)* **12**,
9 doi:10.3390/cancers12123840 (2020).
- 10 11 Busonero, C., Leone, S., Klemm, C. & Acconcia, F. A functional drug re-purposing screening
11 identifies carfilzomib as a drug preventing 17beta-estradiol: ERalpha signaling and cell
12 proliferation in breast cancer cells. *Mol Cell Endocrinol* **460**, 229-237,
13 doi:10.1016/j.mce.2017.07.027 (2018).
- 14 12 Busonero, C. L., S.; Bianchi, F.; Acconcia, F. In silico screening for ER α downmodulators
15 identifies thioridazine as an anti-proliferative agent in primary, 4OH-tamoxifen-resistant and
16 Y537S ER α -expressing breast cancer cells. *Cellular oncology*, doi:10.1007/s13402-018-
17 0400-x (2018).
- 18 13 Cipolletti, M., Leone, S., Bartoloni, S., Busonero, C. & Acconcia, F. Real-time measurement
19 of E2: ERalpha transcriptional activity in living cells. *J Cell Physiol*, doi:10.1002/jcp.29565
20 (2020).
- 21 14 Leone, S., Busonero, C. & Acconcia, F. A high throughput method to study the physiology of
22 E2:ERalpha signaling in breast cancer cells. *J Cell Physiol* **233**, 3713-3722,
23 doi:10.1002/jcp.26251 (2018).
- 24 15 Acconcia, F. *et al.* The extra-nuclear interactome of the estrogen receptors: implications for
25 physiological functions. *Mol Cell Endocrinol* **538**, 111452, doi:10.1016/j.mce.2021.111452
26 (2021).
- 27 16 Cipolletti, M., Leone, S., Bartoloni, S. & Acconcia, F. A functional genetic screen for
28 metabolic proteins unveils GART and the de novo purine biosynthetic pathway as novel
29 targets for the treatment of luminal A ERalpha expressing primary and metastatic invasive
30 ductal carcinoma. *Front Endocrinol (Lausanne)* **14**, 1129162,
31 doi:10.3389/fendo.2023.1129162 (2023).
- 32 17 Pescatori, S. *et al.* Clinically relevant CHK1 inhibitors abrogate wild-type and Y537S mutant
33 ER α expression and proliferation in luminal primary and metastatic breast cancer cells.
34 *Journal of Experimental & Clinical Cancer Research* **41**, 27, doi:10.1186/s13046-022-02360-
35 y (2022).
- 36 18 Neve, R. M. *et al.* A collection of breast cancer cell lines for the study of functionally distinct
37 cancer subtypes. *Cancer cell* **10**, 515-527, doi:10.1016/j.ccr.2006.10.008 (2006).
- 38 19 Dai, X., Cheng, H., Bai, Z. & Li, J. Breast Cancer Cell Line Classification and Its Relevance
39 with Breast Tumor Subtyping. *J Cancer* **8**, 3131-3141, doi:10.7150/jca.18457 (2017).
- 40 20 Techer, H. & Pasero, P. The Replication Stress Response on a Narrow Path Between Genomic
41 Instability and Inflammation. *Front Cell Dev Biol* **9**, 702584, doi:10.3389/fcell.2021.702584
42 (2021).
- 43 21 Bhola, N. E. *et al.* Kinome-wide functional screen identifies role of PLK1 in hormone-
44 independent, ER-positive breast cancer. *Cancer Res* **75**, 405-414, doi:10.1158/0008-
45 5472.CAN-14-2475 (2015).
- 46 22 Bhola, N. E. *et al.* Correction: Kinome-wide Functional Screen Identifies Role of PLK1 in
47 Hormone-Independent, ER-Positive Breast Cancer. *Cancer Res* **79**, 876, doi:10.1158/0008-
48 5472.CAN-18-4088 (2019).
- 49 23 Bartoloni, S., Leone, S. & Acconcia, F. Unexpected Impact of a Hepatitis C Virus Inhibitor
50 on 17beta-Estradiol Signaling in Breast Cancer. *International journal of molecular sciences*
51 **21**, doi:10.3390/ijms21103418 (2020).

- 1 24 Bartoloni, S., Leone, S., Pescatori, S., Cipolletti, M. & Acconcia, F. The antiviral drug
2 telaprevir induces cell death by reducing FOXA1 expression in estrogen receptor alpha
3 (ERalpha)-positive breast cancer cells. *Mol Oncol* **16**, 3568-3584, doi:10.1002/1878-
4 0261.13303 (2022).
- 5 25 Harrod, A. *et al.* Genomic modelling of the ESR1 Y537S mutation for evaluating function
6 and new therapeutic approaches for metastatic breast cancer. *Oncogene* **36**, 2286-2296,
7 doi:10.1038/onc.2016.382 (2017).
- 8 26 Harrod, A. *et al.* Genome engineering for estrogen receptor mutations reveals differential
9 responses to anti-estrogens and new prognostic gene signatures for breast cancer. *Oncogene*
10 **41**, 4905-4915, doi:10.1038/s41388-022-02483-8 (2022).
- 11 27 Finetti, P. *et al.* Sixteen-kinase gene expression identifies luminal breast cancers with poor
12 prognosis. *Cancer Res* **68**, 767-776, doi:10.1158/0008-5472.CAN-07-5516 (2008).
- 13 28 Lanczky, A. & Gyorffy, B. Web-Based Survival Analysis Tool Tailored for Medical Research
14 (KMplot): Development and Implementation. *J Med Internet Res* **23**, e27633,
15 doi:10.2196/27633 (2021).
- 16 29 Toure, B. B. *et al.* Toward the Validation of Maternal Embryonic Leucine Zipper Kinase:
17 Discovery, Optimization of Highly Potent and Selective Inhibitors, and Preliminary Biology
18 Insight. *Journal of medicinal chemistry* **59**, 4711-4723, doi:10.1021/acs.jmedchem.6b00052
19 (2016).
- 20 30 Klionsky, D. J. *et al.* Guidelines for the use and interpretation of assays for monitoring
21 autophagy. *Autophagy* **8**, 445-544, doi:10.4161/auto.19496 (2012).
- 22 31 Creighton, C. J. The molecular profile of luminal B breast cancer. *Biologics* **6**, 289-297,
23 doi:10.2147/BTT.S29923 (2012).
- 24 32 Ali, S., Metzger, D., Bornert, J. M. & Chambon, P. Modulation of transcriptional activation
25 by ligand-dependent phosphorylation of the human oestrogen receptor A/B region. *EMBO J*
26 **12**, 1153-1160, doi:not available. PMID: 8458328. (1993).
- 27 33 Langhans, S. A. Three-Dimensional in Vitro Cell Culture Models in Drug Discovery and Drug
28 Repositioning. *Front Pharmacol* **9**, 6, doi:10.3389/fphar.2018.00006 (2018).
- 29 34 Bartlett, J. M. S. & Parelukar, W. Breast cancers are rare diseases-and must be treated as such.
30 *NPJ breast cancer* **3**, 11, doi:10.1038/s41523-017-0013-y (2017).
- 31 35 Duong-Ly, K. C. & Peterson, J. R. The human kinome and kinase inhibition. *Curr Protoc*
32 *Pharmacol* **Chapter 2**, Unit2 9, doi:10.1002/0471141755.ph0209s60 (2013).
- 33 36 Totta, P., Busonero, C., Leone, S., Marino, M. & Acconcia, F. Dynamin II is required for
34 17beta-estradiol signaling and autophagy-based ERalpha degradation. *Scientific reports* **6**,
35 23727, doi:10.1038/srep23727 (2016).
- 36 37 Korolchuk, V. I., Mansilla, A., Menzies, F. M. & Rubinsztein, D. C. Autophagy inhibition
37 compromises degradation of ubiquitin-proteasome pathway substrates. *Mol Cell* **33**, 517-527,
38 doi:10.1016/j.molcel.2009.01.021 (2009).
- 39 38 Liu, W. J. *et al.* p62 links the autophagy pathway and the ubiquitin-proteasome system upon
40 ubiquitinated protein degradation. *Cell Mol Biol Lett* **21**, 29, doi:10.1186/s11658-016-0031-z
41 (2016).
- 42 39 Laios, I. *et al.* Role of the proteasome in the regulation of estrogen receptor alpha turnover
43 and function in MCF-7 breast carcinoma cells. *J Steroid Biochem Mol Biol* **94**, 347-359,
44 doi:10.1016/j.jsbmb.2005.02.005 (2005).
- 45 40 Gettinger, S. N. *et al.* Activity and safety of brigatinib in ALK-rearranged non-small-cell lung
46 cancer and other malignancies: a single-arm, open-label, phase 1/2 trial. *Lancet Oncol* **17**,
47 1683-1696, doi:10.1016/S1470-2045(16)30392-8 (2016).
- 48 41 Cipolletti, M., Pescatori, S. & Acconcia, F. Real-time challenging of ER α Y537S mutant
49 transcriptional activity in living cells. *Endocrines* **2**, 54-64, doi:10.3390/endocrines2010006
50 (2021).

- 1 42 Totta, P., Pesiri, V., Enari, M., Marino, M. & Acconcia, F. Clathrin Heavy Chain Interacts
2 With Estrogen Receptor alpha and Modulates 17beta-Estradiol Signaling. *Mol Endocrinol* **29**,
3 739-755, doi:10.1210/me.2014-1385 (2015).
- 4 43 Pesiri, V., Totta, P., Marino, M. & Acconcia, F. Ubiquitin-activating enzyme is necessary for
5 17beta-estradiol-induced breast cancer cell proliferation and migration. *IUBMB Life* **66**, 578-
6 585, doi:10.1002/iub.1296 (2014).

7

Figure 1

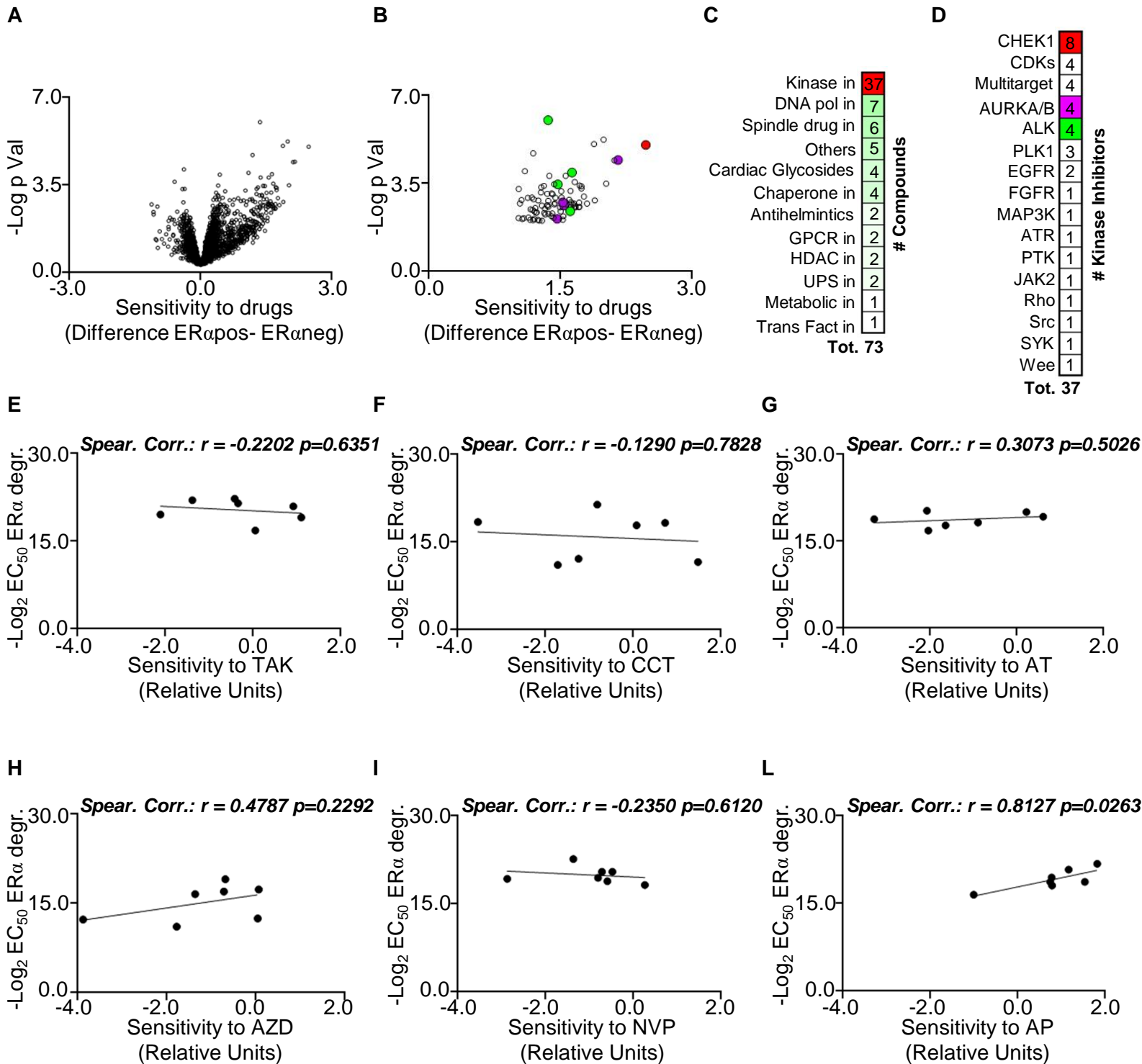
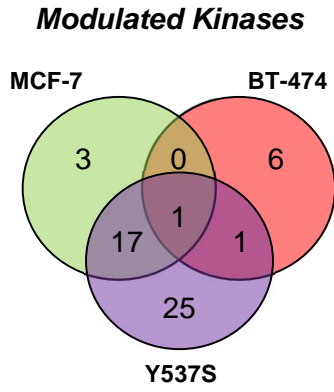
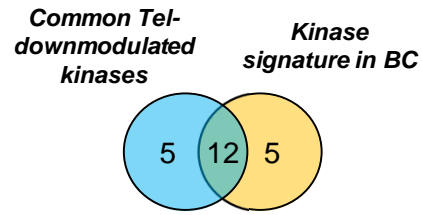


Figure 2

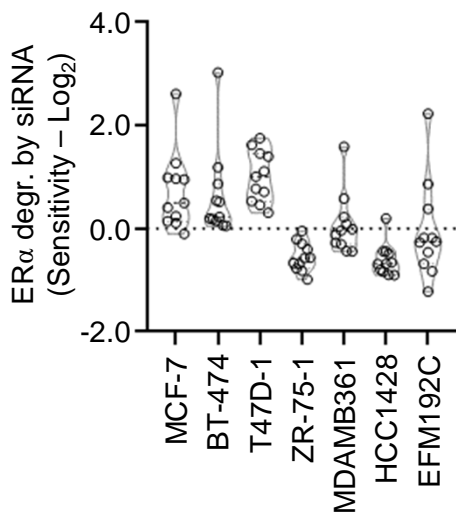
A



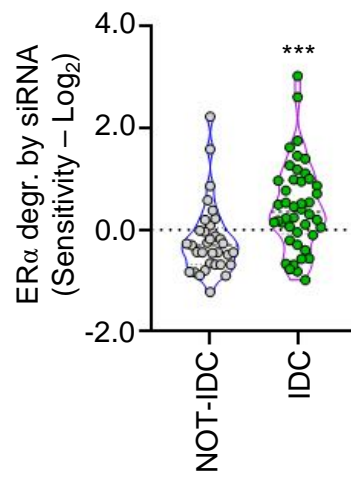
B



C



D



E

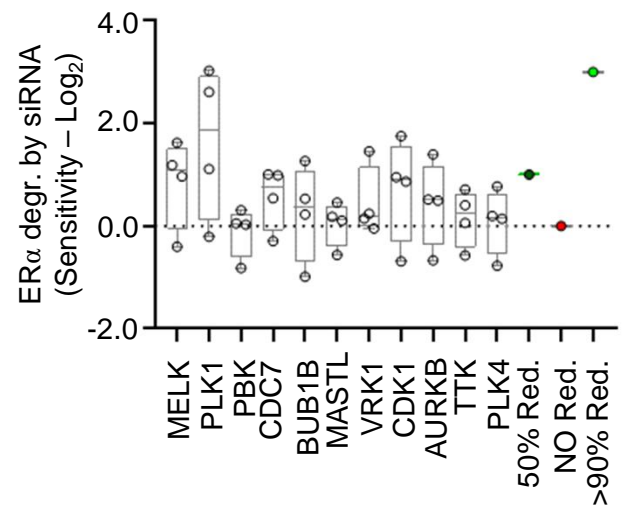
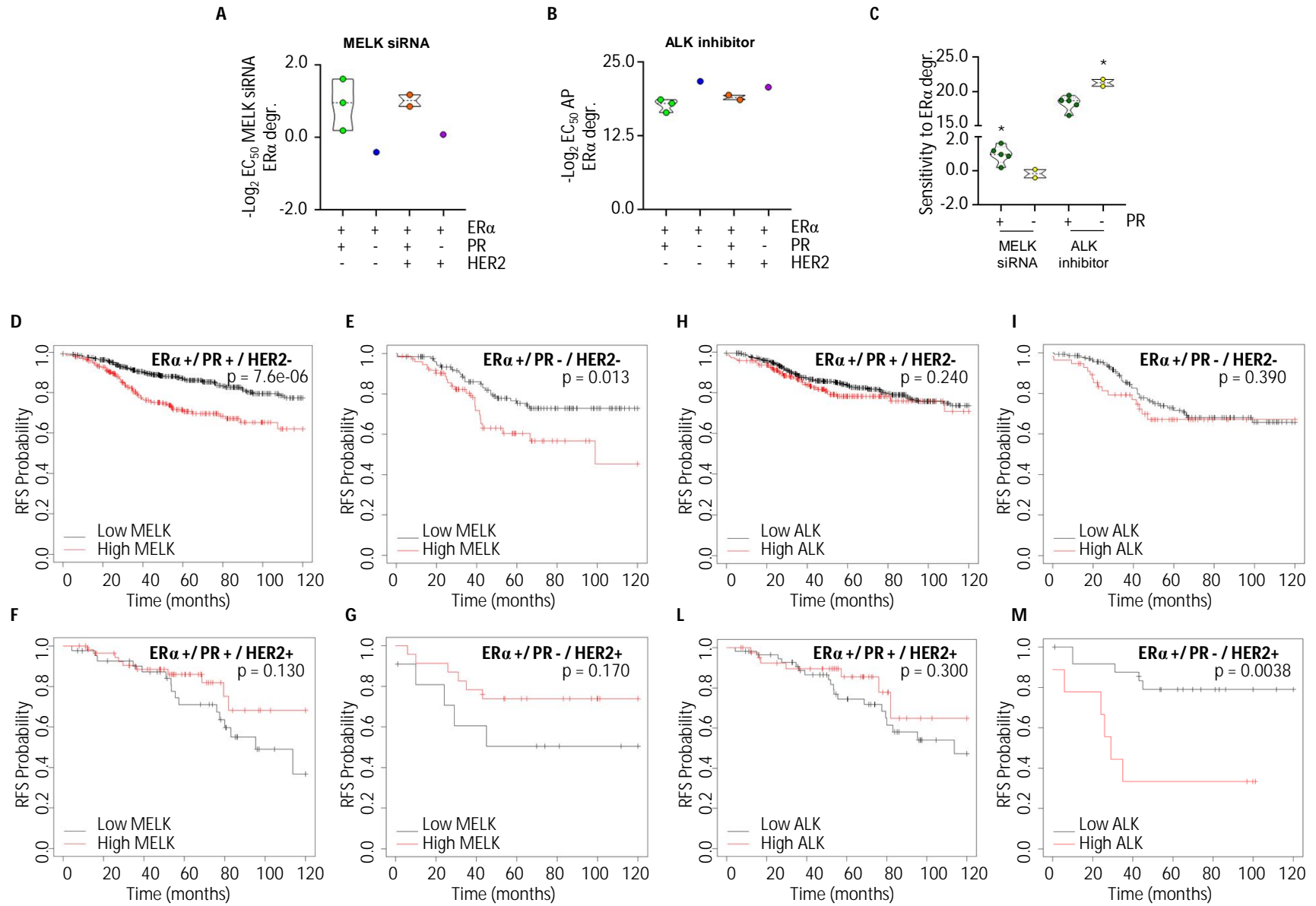
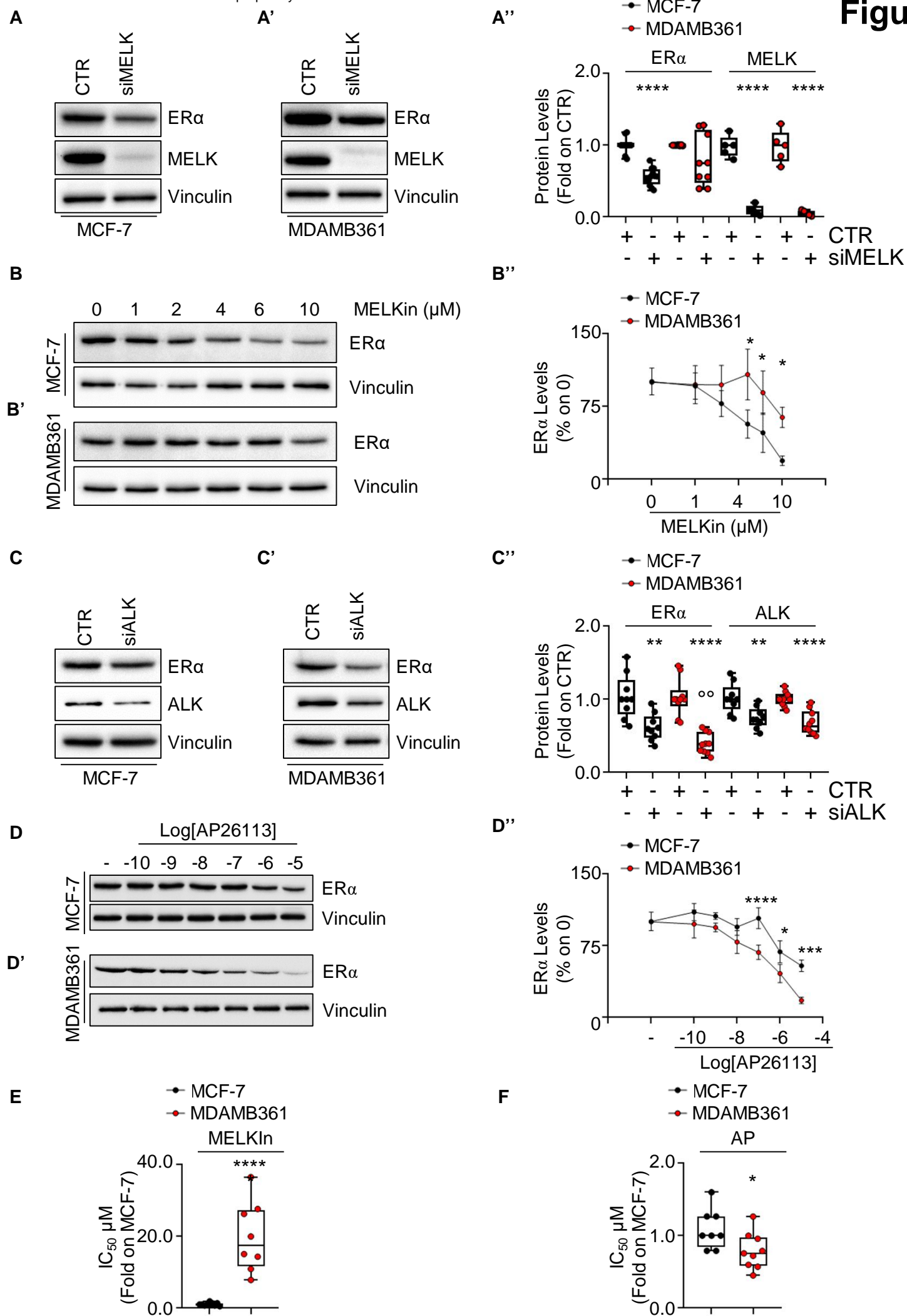


Figure 3





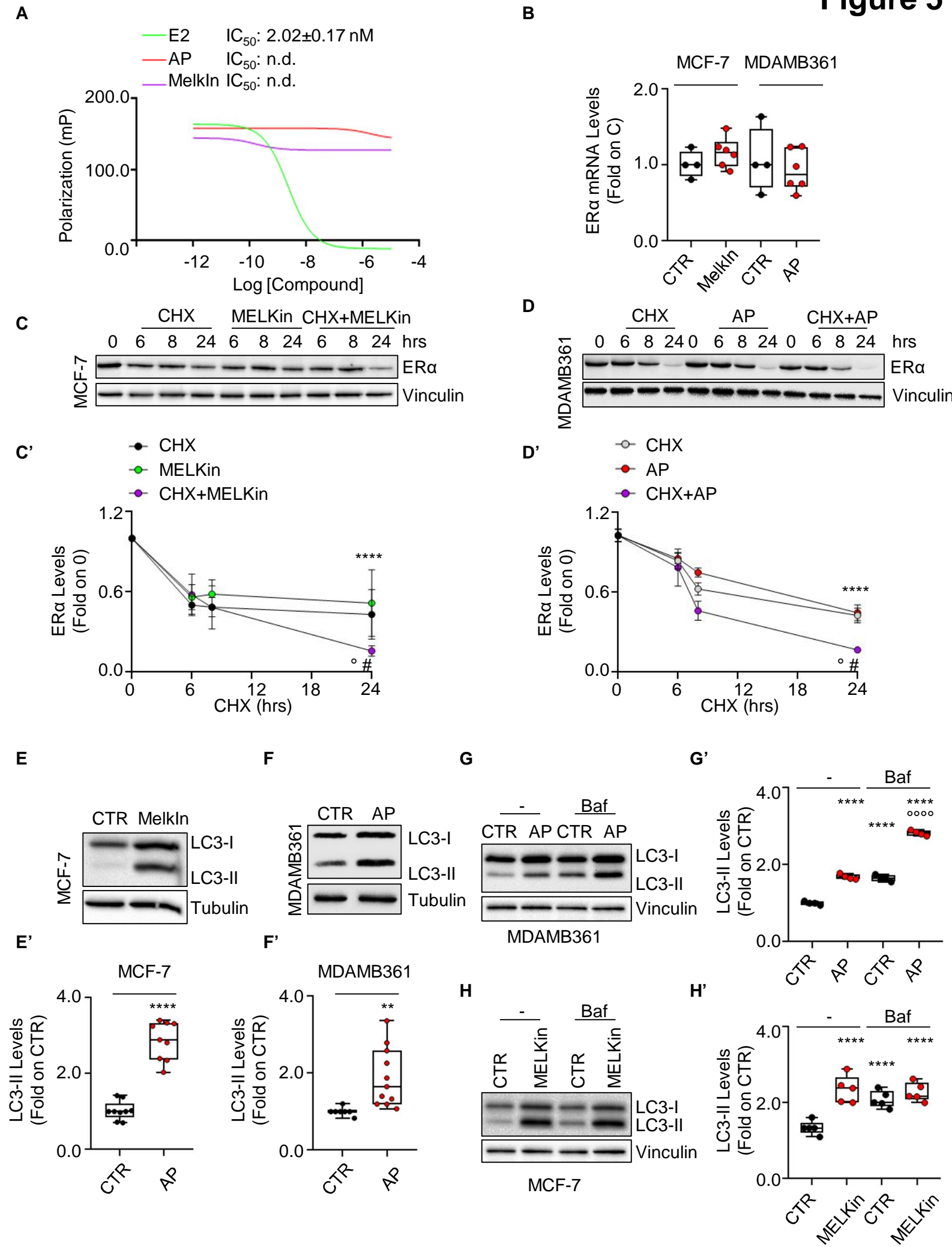


Figure 6

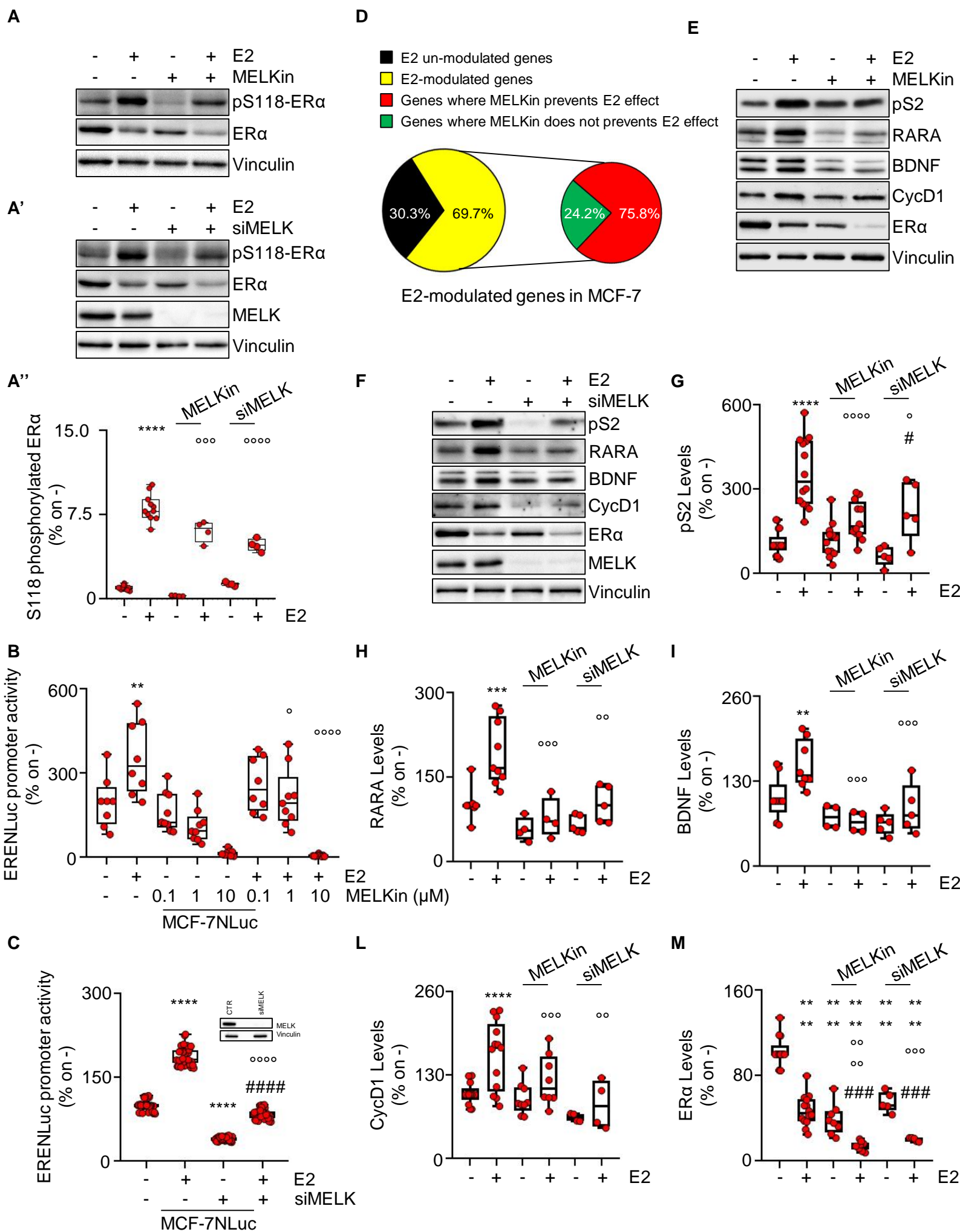
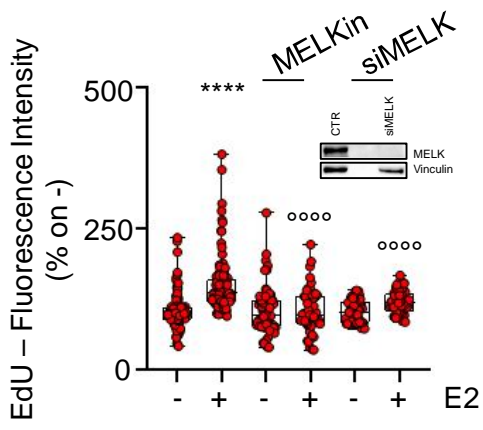


Figure 7

A



B

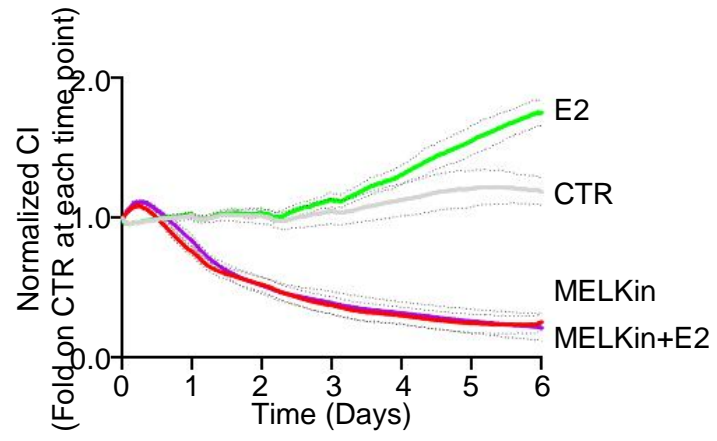
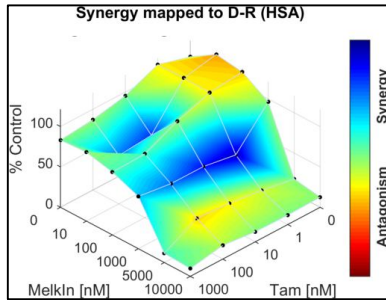
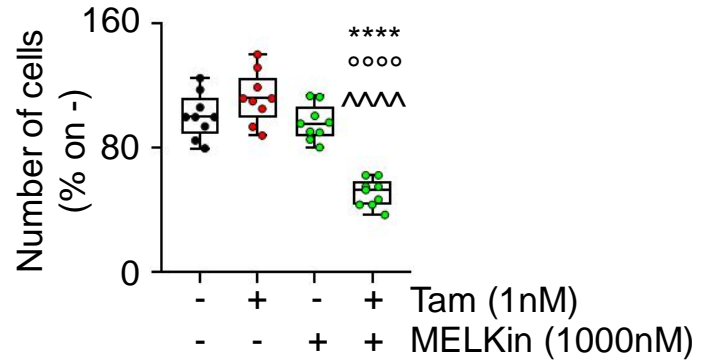


Figure 8

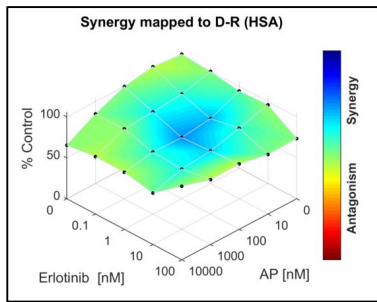
A



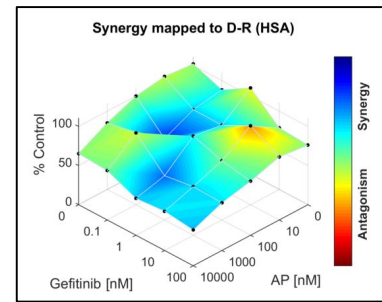
A'



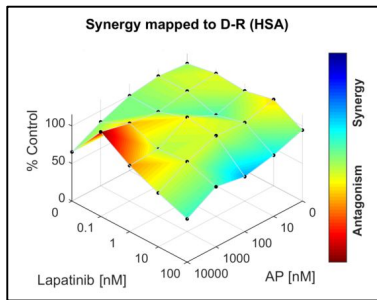
B



C



D



E

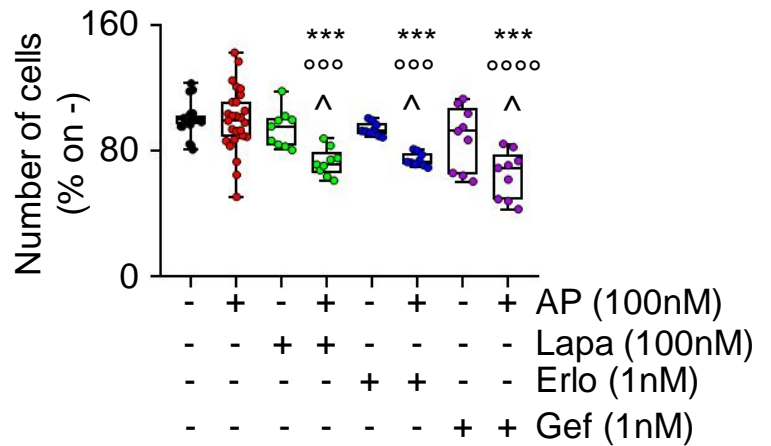
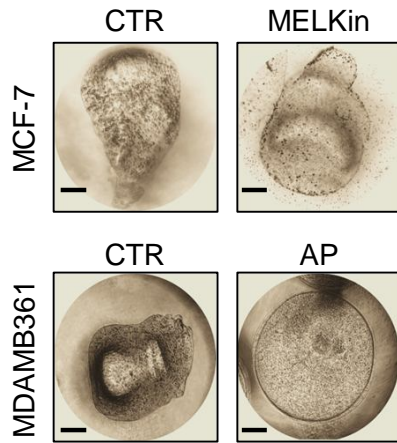
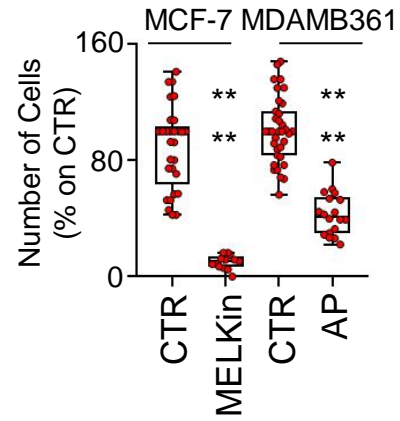


Figure 9

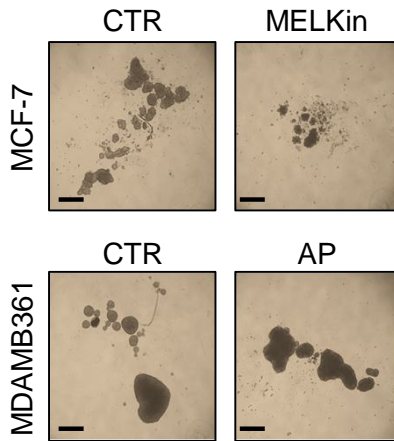
A



A'



B



B'

